Marine Geology

Sr isotope variations in Oligocene–Miocene and modern biogenic carbonate formations of Koko Guyot (Emperor Seamount Chain, Pacific Ocean)

--Manuscript Draft--

Manuscript Number:	MARGO-D-22-00055R2
Article Type:	Research Paper
Keywords:	87Sr/86Sr ratio, δ88/86Sr, Corals, Bryozoans, Larger foraminifera, Subsidence, Hawaiian-Emperor Seamount Chain, Hawaiian hotspot
Corresponding Author:	Irina Andreevna Vishnevskaya, Ph.D. Institut geohimii i analiticeskoj himii imeni V I Vernadskogo Rossijskoj akademii nauk Moscow, RUSSIAN FEDERATION
First Author:	Irina Andreevna Vishnevskaya, Ph.D.
Order of Authors:	Irina Andreevna Vishnevskaya, Ph.D.
	Marc Humblet, PhD
	Yasufumi Iryu, PhD
	Davide Bassi, PhD
	Tatiana G. Okuneva
	Daria V. Kiseleva, PhD
	Andrey V. Vishnevskiy, PhD
	Natalia G. Soloshenko
	Pavel E. Mikhailik, PhD
Abstract:	The Hawaiian–Emperor Seamount Chain, a major topographic feature of the Pacific Ocean floor, is composed of seamounts capped with fossil coral reef deposits that originally formed close to sea level but are now covered by hundreds of meters of water owing to prolonged subsidence. These fossil reef deposits are important archives of paleoenvironmental change and yield information on the subsidence history of the seamounts. We studied the Sr isotope compositions of Oligocene–Miocene coral reef limestone from Koko Guyot in the southern Emperor Seamount Chain to assess the dynamics of the subsidence. The ages of the studied samples containing coral fragments established by Sr isotope stratigraphy vary from 26.3 to 20.1 Ma. In contrast, the youngest samples (15.3 Ma), which were deposited in water depths of >120 m, are barren of corals and are composed exclusively of bryozoans and coralline algae. The subsidence rate of the Koko Guyot volcanic structure was not constant over time. Integration of our new data with the results of previous studies reveals that the subsidence rate was 0.046 ± 0.005 mm/yr during the first 25–30 Myr (from 49–44 to 20 Ma). During this period, Koko Guyot was in a bathymetric interval favorable for coral reef development, and its subsidence was compensated by rapid vertical growth of the reef. Subsequently, the subsidence rate decreased to an average value of 0.019 ± 0.003 mm/yr from 20 to 15 Ma. The decrease in the rate of bottom subsidence coincided with unfavorable environmental conditions for coral reef development, leading to the disappearance of corals. The average subsidence rate has been 0.015 ± 0.002 mm/yr since 15 Ma, comparable to the present-day subsidence rate. We also analyzed the stable Sr isotope ratios (δ 88/86 Sr) of warm-water coral samples formed at 25–20 Ma (0.32‰ ± 0.1‰), as well as carbonate of large benthic foraminifera, coralline algae, and other non-coral species for the period 20–15 Ma (0.10‰ ± 0.09‰). We suggest that the large difference in carbonate δ 88/86 Sr between 25–20 and 20–15 Ma corresponds to a difference in the fractionation factor caused by environmental and benthic community change.
Suggested Reviewers:	John McArthur, PhD Prof, UCL: University College London j.mcarthur@ucl.ac.uk Specialist on Sr-isotope stratigraphy

	Jay L. Banner, PhD Prof, University of Texas at Dallas banner@mail.utexas.edu Specialist on Sr-isotope stratigraphy
	Alan Kaufman, PhD Prof, University of Maryland Center for Environmental Science kaufman@umd.edu Specialist on Sr-isotope stratigraphy
	Sarah Smith, PhD Prof, University of California Museum of Paleontology sarahsmith@ucsd.edu Specialist on paleontology
	Yukiko Kozaka, PhD Prof, University of Toyama: Toyama Daigaku horikawa@sci.u-toyama.ac.jp Specialist on isotopic geochemistry of seawater
	Kazuyo Tachikawa, PhD Prof, Aix-Marseille I University: Aix-Marseille Universite kazuyo@cerege.fr Specialist on isotopic geochemistry of seawater
Response to Reviewers:	

Dear Editor and Reviewer,

Thank you very much for your review of our manuscript titled "Sr isotope variations in Oligocene–Miocene and modern biogenic carbonate formations of Koko Guyot (Emperor Seamount Chain, Pacific Ocean)". We have revised our article and would like to present it to you.
Some comments had incorrect line numbers. We found what they referred to and signed the correct line numbers in the answers.
We submitted the text for professional proofreading to Stallard Scientific Editing, where we corrected the entire text. We left the grammatical and punctuation corrections in the file with marks. Following their recommendations, we improved the understanding of Fig. 1,4, 5, 6 and tables 1 and 2.
Also, throughout the text we have changed "biocommunity" to "benthic community" because this is more paleontological correct.
Below are the responses to your comments.

Response to the Reviewer #1's comments:

Line 47-52 - Suggested revision: "We also analyzed the stable Sr isotope ratios (d88/86Sr) of warm-water coral samples formed 25-20 Ma ago (0.32±0.1‰) and more recent carbonate composed of Larger benthic foraminifera, and coralline algal, and other non-coral species from 20-15 Ma (0.10±0.09‰). We suggest that the large difference in carbonate d88/86Sr between these two intervals corresponds to a difference in fractionation factor due to environmental and biocommunity change." - **corrected**

Line 73 - Moving the geological background information for Koko Guyot to the following section was helpful for readability, but you need to check that the necessary introductory information is still provided here (specifically, you do not transition from discussing the Emperor Seamount Chain generally to your description of reef growth on Koko Guyot). Add a condensed description of Koko Guyot here before you begin referring to it specifically in Line 96. **– corrected.**

Line 120 - Good additional description of novelty (new sampling method); in 122-124, I suggest rephrasing to: "Our purpose was to confirm the previous estimates by Clague et al. (2010) with samples taken from a site remote from the area of previous work and, if possible, improve them by…." (Explain specifically how they could be improved; reducing uncertainty?). – **corrected in lines 98-101**

Line 139 -169 - Check organization of these paragraphs now that you have moved information from the introduction to this section; you refer to Koko Guyot in the first paragraph, and then reintroduce it in the second. Rewrite to avoid redundancy. **Lines 120-143**

Line 224 - Clarify: other studies have used both TIMS and MC-ICP-MS to measure stable Sr. Here it initially sounds as though you used both methods in this study. "… have been measured in other studies using both…" – **corrected in line 197**

Line 309 - Clarify: The ratio of 88Sr/86Sr in carbonates depends on the 88Sr/86Sr ratio of seawater, which changes through time due to variation in the same fluxes that control seawater 87/86 as well as the net carbonate flux from the ocean, and the degree of fractionation between seawater and carbonate, which depends on species and temperature. This is important to distinguish because when you compare your data to the Paytan et al. 2021 curve, it is the offset between the seawater curve and your data that may tell you something about changes in species/environment (that is, I would not necessarily expect your carbonate values to line up with the seawater values but rather be offset by some constant (or variable) fractionation factor). - **corrected in line 277**

Line 313- Rephrase: "Minerals like carbonate formed in seawater are generally characterized by lower d88/86Sr because of seawater-mineral fractionation. Moreover, minerals of chemogenic and biogenic origins can be distinguished by the degree of their stable Sr isotope fractionation (Fietzke and Eisenhauer, 2006; Fruchter et al., 2016) which may depend on temperature and varies for different species. Thus..." **corrected in lines 280-283**

Line 324 - Without a conceptual framework for the direction of change you expect to see, the stable Sr data is not all that useful for inferring anything about the nature of the species transition or environmental shift. I do think that your revisions somewhat (rightly) de-emphasized the use of stable Sr isotopes as a diagnostic tool for environmental change in this setting. Rather, you have generally tested the idea that a community shift you have independently inferred (i.e., reef assemblages replaced by cold water species) might have an impact on stable Sr isotopes (because of the known dependencies of the seawater-carbonate fractionation factor on species and temperature that you introduce above). I suggest that you rewrite Line 324-325 to explain that within the scope of this study, you are looking to see if d88/86Sr of your specific samples shift in relation to the subsidence and migration of the guyot and subsequent environmental changes, but in this case the d88/86Sr measurements do not provide an independent proxy for these changes and there are many factors that complicate their interpretation. **corrected in lines 290-292**

Line 357 - Rephrase: "Because secondary processes have been shown to alter the initial d88/86Sr of carbonates, we use only the three samples that are the least modified in our discussion." **corrected in lines 318-320**

Line 361 - Specify what the agreement between the carbonate samples d88/86Sr and seawater curve indicates (these particular carbonate samples apparently fractionated very little from seawater?). It is important to note that you don't necessarily expect the carbonate values to line up with the seawater values, and then explain why these might. Add explanations to address these questions: The error bar is quite large, but is it possible that these have in fact undergone some alteration (would this lead to increased d88/86Sr values relative to initial composition)? Is there evidence in the literature that the assemblages you expect to be represented by these samples would fractionate <0.09‰ from seawater? Are these non-representative samples, possibly explaining why Lv86-9-6 is slightly different (though within error) compared to the other two? You should more thoroughly present the possible complications here. - **corrected in line 321,**

Line 369 - Specify that in the absence of significant changes in seawater d88/86Sr, the dramatic difference between carbonate and seawater in this interval likely indicates larger fractionation between seawater and carbonate compared to the earlier interval. Then you can hypothesize what might be driving this fractionation. **corrected in line 323.**

Line 371 - Start new paragraph and revise for clarity: "Biocommunity alteration to much more cool water resistance can be correlated with the bottom subsidence rate and guyot migration to higher latitudes (Wilson, 1963; Clague and Dalrymple, 1987; Tarduno et al., 2003; Clague et al., 2010). The change in the temperature and light regime as Koko Guyot subsided and migrated led to biocommunity alteration as reef benthic assemblages were replaced as the dominant species by larger foraminiferal species. We suppose that this biocommunity transition is expressed in the dramatic decrease of δ88/86Sr in our samples (Fig. 4) in the absence of major changes in seawater δ88/86Sr." **corrected in lines 324-329.**

Line 377 - Move sentence about modern echinoid d88/86Sr values to Line 371 before new paragraph and add comparison of the fractionation between seawater-echinoid today vs. seawater-carbonate from 20 to 15 Ma. **corrected in line 330.**

Line 378 - I don't think you have enough information to draw this broad conclusion. Rather, you can simply say that you observe a shift in the d88/86Sr of your samples that seems to coincide with the biocommunity transition, suggesting the fractionation factor possibly changed along with environmental factors (temperature, dominant species) as might generally be expected. However, complicating factors (be specific) limit further interpretation of these data. **corrected in line 331.**

Line 447 - See Line 378 comment above and revise. **- corrected in lines 398-401.**

Line 461 - In your introduction, you note that you hoped to improve the prior estimates. Summarize the specific advance and how these new rates fit into the overall picture of Pacific subsidence. That is, tell us specifically how "The data obtained refine the existing models of subsidence of the Pacific crust." **- corrected in lines 412-413.**

We would like to thank Editor-in-Chief of Marine Geology Dr. Adina Paytan and anonymous reviewers for their thorough comments and suggestions, which have improved our manuscript.

Sincerely yours,

Irina Vishnevskaya

Highlights for paper Vishnevskaya et al., “Sr isotope variations …”

The subsidence rate of Koko Guyot was not uniform

The age of corals and larger foraminiferal species was determined by strontium isotope stratigraphy.

The study of strontium isotope composition showed that the least altered limestones containing the fragments of reef corals were formed in the early Miocene

Graphical Abstract

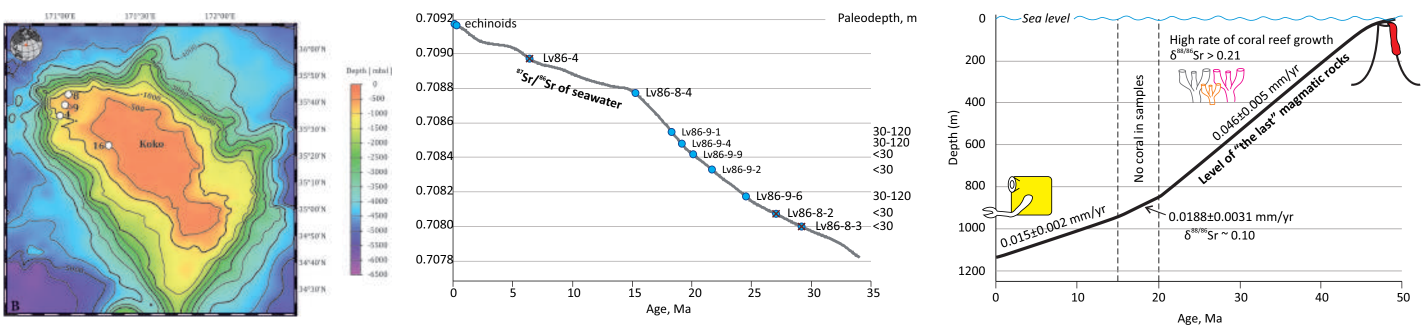

Sr isotope variations in Oligocene–Miocene and modern biogenic carbonate formations of Koko Guyot (Emperor Seamount Chain, Pacific Ocean)

Irina A. Vishnevskaya [a,b,*], Marc Humblet [c], Yasufumi Iryu [d], Davide Bassi [e], Tatiana G. Okuneva [f], Daria V. Kiseleva [f], Andrey V. Vishnevskiy [b, g], Natalia G. Soloshenko [f], Pavel E. Mikhailik [h]

[a] *Vernadsky Institute of Geochemistry and Analytical Chemistry, RAS, 119334 Moscow, 19 Kosygina str., Russia*
[b] *Novosibirsk State University, 630090 Novosibirsk, 1 Pirogova str., Russia*
[c] *Nagoya University, Department of Earth and Planetary Sciences, 464-8601 Nagoya, Japan*
[d] *Institute of Geology and Paleontology, Graduate School of Science, Tohoku University, Aramaki-aza-aoba 6-3, Aoba-ku, Sendai 980-8578, Japan*
[e] *Dipartimento di Fisica e Scienze della Terra, Università degli Studi di Ferrara, Via Saragat 1, I-44122, Ferrara, Italy*
[f] *Zavaritsky Institute of Geology and Geochemistry, UB RAS, 620016 Ekaterinburg, 15 Akademika Vonsovskogo str., Russia*
[g] *Sobolev Institute of Geology and Mineralogy, SB RAS, 630090 Novosibirsk, 3 Akademika Koptyuga ave., Russia*
[h] *Far East Geological Institute, Far East Branch of Russian Academy of Sciences (FEGI FEB RAS), Prospekt 100-letiya, 159, 690022 Vladivostok, Russia*

* Corresponding author:
E-mail address: vishnevskaia@geokhi.ru, vishnevskaia.i.a@gmail.com (I.A. Vishnevskaya).

ABSTRACT

The Hawaiian–Emperor Seamount Chain, a major topographic feature of the Pacific Ocean floor, is composed of seamounts capped with fossil coral reef deposits that originally formed close to sea level but are now covered by hundreds of meters of water owing to prolonged subsidence. These fossil reef deposits are important archives of paleoenvironmental change and yield information on the subsidence history of the seamounts. We studied the Sr isotope compositions of Oligocene–Miocene coral reef limestone from Koko Guyot in the southern Emperor

Seamount Chain to assess the dynamics of the subsidence. The ages of the studied samples containing coral fragments established by Sr isotope stratigraphy vary from 26.3 to 20.1 Ma. In contrast, the youngest samples (15.3 Ma), which were deposited in water depths of >120 m, are barren of corals and are composed exclusively of bryozoans and coralline algae. The subsidence rate of the Koko Guyot volcanic structure was not constant over time. Integration of our new data with the results of previous studies reveals that the subsidence rate was 0.046 ± 0.005 mm/yr during the first 25–30 Myr (from 49–44 to 20 Ma). During this period, Koko Guyot was in a bathymetric interval favorable for coral reef development, and its subsidence was compensated by rapid vertical growth of the reef. Subsequently, the subsidence rate decreased to an average value of 0.019 ± 0.003 mm/yr from 20 to 15 Ma. The decrease in the rate of bottom subsidence coincided with unfavorable environmental conditions for coral reef development, leading to the disappearance of corals. The average subsidence rate has been 0.015 ± 0.002 mm/yr since 15 Ma, comparable to the present-day subsidence rate. We also analyzed the stable Sr isotope ratios ($\delta^{88/86}$Sr) of warm-water coral samples formed at 25–20 Ma (0.32‰ ± 0.1‰), as well as carbonate of large benthic foraminifera, coralline algae, and other non-coral species for the period 20–15 Ma (0.10‰ ± 0.09‰). We suggest that the large difference in carbonate $\delta^{88/86}$Sr between 25–20 and 20–15 Ma corresponds to a difference in the fractionation factor caused by environmental and benthic community change.

Key words:
^{87}Sr/^{86}Sr ratio, $\delta^{88/86}$Sr, Corals, Bryozoans, Larger foraminifera, Subsidence, Hawaiian–Emperor Seamount Chain, Hawaiian hotspot

1. Introduction

The Emperor Seamount Chain (Pacific Ocean) includes more than a dozen seamounts (i.e., extinct volcanoes). The northernmost seamount of Meiji is considered the oldest, with an age estimated at 85 Ma (Keller et al., 2000). The youngest seamount of Daikakuji (42 Ma; Dalrymple and Clague, 1976) is located at the junction of the Emperor Seamount Chain with the Hawaiian Seamount Chain (Fig. 1). Koko Guyot is the southernmost seamount and one of the largest in the Emperor Seamount Chain, with a surface area of 5800 km^2 (Greene et al., 1980). This guyot is located from 34°N to 36.5°N and from 170.8°E to 171.5°E. The top of the guyot is positioned at a minimum depth of 270 m below sea level (Matter, Gardner, 1975) and is characterized by a predominantly flat upper surface at 300–400 m water depth.

The Emperor–Hawaiian Seamount Chain formed as a result of the prolonged activity of the so-called Hawaiian hotspot, a long-lived mantle plume beneath the Pacific Plate (Jackson et al., 1980; Clague and Dalrymple, 1987; Tarduno et al., 2003; and references therein). Plate movement relative to conventionally stationary mantle structure led to the formation of a linear chain of volcanic islands and seamounts with ages increasing from south to north. The seamounts situated in the southern Emperor Seamount Chain are topped with a sediment cover containing carbonate rocks (Shipboard Scientific Party, 1975a, 1975b, 2002), which represent an excellent record of geochemical, paleontological, and paleogeographic settings.

The following development sequence for seamounts has been established (Wheeler and Aharon, 1991). After the cessation of volcanic activity, a coral reef began to develop on the volcanic island. Over time, the volcano subsided, and the coral reef at first kept pace with relative sea-level rise by enlarging upward. As the oceanic crust moved away from the area of plume activity and cooled, the volcano subsided further, and the coral reef (which was unable to keep up with sea-level rise) drowned. Although the main cause of the demise of the coral was the rapid relative sea-level rise, other factors such as a decrease in sea surface temperature as the volcanic island migrated to higher latitudes by plate motion may also have been influential (e.g., Clague et al., 2010).

Data regarding the speed and direction of movement of the Hawaiian hotspot and the Pacific Plate show that the paths of Koko Guyot and the hotspot diverged (*c*. 45 Ma), whereby the seamount moved to the north and the hotspot moved to the south (Wilson, 1963; Clague and Dalrymple, 1987; Tarduno et al., 2003). Clague et al. (2010) studied corals in southern Koko Guyot and used Sr isotope stratigraphy to date the carbonates. According to those authors' calculations, Koko Guyot migrated northward at a rate of 69 km/Myr during the first 5 Myr (*c.* 50–45 Ma) of its existence, moving from 21.5° to 23°N. In addition, the rate at which the guyot migrated decreased to 31 km/Myr between 45 Ma and the present, and the direction of movement changed to the northwest before reaching its present position at 35°N. Clague et al. (2010) proposed a two-phase subsidence history for Koko Guyot: (1) ~0.009 mm/yr from 27.1 to 16.2 Ma; and (2) ~0.014 mm/yr from 16.2 Ma to the present. Those authors also suggested that the timing of reef growth cessation at Koko Guyot occurred at *c.* 29 Ma, on the basis of the youngest age of sampled corals (27 Ma) and the calculated average subsidence rate (0.012 mm/yr).

We studied samples obtained from the northwestern part of Koko Guyot, where sampling has hitherto not been conducted. We used a new sampling method for this region, namely, a remotely controlled underwater vehicle (see "Material and Methods"), so our samples could be geographically and bathymetrically referenced. Our purpose was to confirm the previous estimates of coral age and subsidence rate made by Clague et al. (2010) with samples taken from a site distant from the area of previous work and, if possible, improve the estimates by measuring isotope ratios using a different type of equipment (a Neptune Plus multicollector inductively coupled plasma mass spectrometry (ICP–MS) instrument versus a VG Sector 54 Thermal ionization mass spectrometer (TIMS) in Clague et al. (2010)) and reducing uncertainties in age estimates. The aim of the study was to establish the youngest age limit of coral reefs on Koko Guyot and further constrain the timing of coral reef drowning as Koko Guyot became submerged. In addition, to improve the understanding of the subsidence history of Koko Guyot, we used differences in the ages of sampled corals and their depths to calculate the average subsidence rate of this volcanic structure for different periods. To achieve these aims, we performed paleontological analysis and measured the Sr isotope compositions of samples collected from the Koko Guyot. We compared the obtained $^{87}Sr/^{86}Sr$ ratios with the variation curve of this ratio for the Cenozoic (McArthur et al., 2001, 2020). In addition, we used the $\delta^{88/86}Sr$ record measured in carbonates as a proxy for environmental change on the flooded reef platform.

2. Materials and methods

The 86th voyage of the research vessel "Akademik M.A. Lavrentiev" was held during July–August 2019. The aim of the expedition was to conduct a comprehensive study of the seamounts of the southern Emperor Seamount Chain. The subject of the present study, the southernmost and youngest seamount of the Emperor Seamount Chain (i.e., Koko Guyot), is an isolated underwater volcanic seamount with a flat top lying more than 300 m below present mean sea level. The guyot is composed mainly of alkaline basalts with minor tholeiitic basalts (Clague and Dalrymple, 1987). The final stage of eruptions is represented by interlayered pahoehoe flows, subaerial aa units, and flow foot breccias. During the course of previous studies as part of the Deep Sea Drilling Program (DSDP) and Ocean Drilling Program (ODP), several sediment cores were recovered: DSDP Leg 32 sites 308 and 309 (Shipboard Scientific Party, 1975a, 1975b) and ODP Leg 197 Site 1206 (Shipboard Scientific Party, 2002). The materials collected during those expeditions allowed the earliest sedimentation stages and waning of volcanic activity to be investigated, as well as fossil benthic assemblages, paleoenvironmental setting, and ages volcanic and sedimentary rocks. At ODP Site 1206, lava flows are separated by limestone and volcaniclastic sandstone layers (Tarduno et al., 2003), suggesting the near-surface nature of the eruptions. The age of the volcanic edifice of the Koko Guyot is estimated as 49–48 Ma (Jackson et al., 1980; Tarduno et al., 2003; Duncan and Keller, 2004). The minimum age of the Koko eruptions has been determined from nannofossils occurring at the base of the sedimentary cover, which probably overlaps the last lava flow, and coincides with biozones NP14 and NP15 (middle Eocene; Speijer et al., 2020). A seismic survey of the Koko Guyot has shown that the volcanic structure is covered by a ~600-m-thick carbonate cap associated with coral reef deposits (Davies et al., 1972). The exposed sedimentary part of drill cores from DSDP sites 308 and 309 is composed of altered volcanoclastic siltstones and sandstones with a sharp contact between them. The sandstones contain bioclasts of bryozoans, solitary corals, ostracods, coralline algae, benthic foraminifera, mollusks, and ooids. The fossil assemblage indicates an early Eocene shallow-water setting (Larson et al., 1975).

The materials collected for the present study were collected using a remotely operated underwater vehicle (Comanche, SUB-Atlantic, UK), equipped with Schilling Robotics Orion hydraulic manipulators, and a Sonardyne hydroacoustic positioning system coupled with a GPS navigation system. During the voyage, 11 dives were performed to survey the top and slopes of Koko Guyot. Carbonate material was collected during four dives, three of which were performed on the northwestern peak of the guyot (dives 4, 8, and 9; Fig. 1) and the fourth in the western part of the main plateau (dive 16; Fig. 1). A living deep-sea isidid octocoral, also termed “bamboo coral”, was collected during dive 4. We used this octocoral as a reference for modern carbonate accumulation. Sampling points and physical water characteristics are presented in Fig. 1 and Table 1. Carbonate rocks were collected directly with a manipulator operated from the surface (Fig. 2A) and with a 15 cm × 15 cm scoop net (Fig. 2B). For rocks collected by the manipulator, a block measuring 1.5 cm × 1.5 cm × 1.5 cm in size was cut from the central part of each rock sample. These cubes were passed through a magnet to remove any metal shavings from the saw and washed in distilled water. For material collected by the scoop net, the sediment was washed with seawater and sorted into different grain-size fractions from 1 to 50 mm. After careful visual inspection, the lightest-colored and unaltered samples devoid of Fe–Mn oxide–hydroxide coatings were selected for geochemical analyses. The selected samples were washed with a brush in running water and finally rinsed in distilled water. All samples were photographed directly on board.

Further sample preparation was carried out in the cleanrooms (class 1000) and laminar boxes (class 100) of the Laboratory of Physical and Chemical Methods of Analysis, Zavaritsky Institute of Geology and Geochemistry UB RAS, Ekaterinburg, Russia. Fragments of carbonate rocks without an outer crust and individual parts of fossils weighing about 100 mg were washed three times in ultrapure water (AriumPro, Sartorius). Then, 5 ml of 1N HCl were added. Although complete dissolution of all the material occurred during the first few minutes, the samples were left in the acid for 24 h at room temperature. The solution was then centrifuged for

20 min at 6000 rpm in an EBA 21 centrifuge (Hettich, Germany). The resulting supernatant was taken from the central part of the liquid column so that undissolved residue containing the flakes of possible organic matter would not enter the resulting liquid. Measurements showed that Fe and Mn contents were less than 50 ppm and less than 20 ppm in the majority of the samples, respectively. These values are consistent with data for the lattice phases of foraminiferal calcite from Palmer (1985) and provide evidence for the lack of secondary Fe–Mn oxide–hydroxides in the studied solutions. The resulting liquid was divided into two aliquots: 2 ml was transferred to test tubes for elemental analysis, and the rest of the liquid was retained for Sr isotope analysis.

An ICP–atomic emission spectrometry (AES) instrument (Optima-8000 DV, PerkinElmer, USA) was used to determine major-element compositions, including Mg, Mn, Sr, and Al, as well as traces of Fe. Control of the accuracy and precision of major- and trace-element compositions was performed using IAG/CGL 020 ML-3 certified limestone provided by the Central Geological Laboratory of Mongolia. The contents of major and trace elements were measured on a regular basis during 2019, yielding the following contents: Fe = 2350 ± 350 ppm, Al = 6000 ± 900 ppm, Mn = 180 ± 30 ppm, Mg = 8400 ± 1260 ppm, and Sr = 1000 ± 150 ppm (2SD, N = 30). The obtained contents were in good agreement with the certified values of Fe = 2400 ± 100 ppm, Al = 6100 ± 100 ppm, Mn = 178 ± 8 ppm, Mg = 8350 ± 145 ppm, and Sr = 1018 ± 30 ppm (Certificate of analysis IAG / CGL 020 ML-3 (Limestone), 2015). The precision of each individual result (relative standard deviation or RSD) was better than 1%.

The volumes of liquid samples calculated to match ~300 ppb of Sr were placed in a PFA vial and evaporated to dryness on a hotplate at 120 °C. The residue was dissolved in 0.5 mL of 7M HNO_3, placed in an Eppendorf microtube, and centrifuged at 6000 rpm for 15 min by an EBA 21 centrifuge (Hettich, Germany). A single-step chromatography technique using SR-Resin (100–200 mesh, Triskem®, TrisKem International, France) was applied for Sr isolation (Vishnevskaya et al., 2020). Purified Sr fraction was evaporated to dryness and dissolved with 3% HNO_3 (v/v) for further isotope ratio measurement.

Stable Sr isotopic compositions have been measured in other studies using both TIMS and MC–ICP–MS (McArthur et al., 2020; Teng et al., 2017). The double-spike (DS) technique is usually applied for TIMS (Krabbenhöft et al., 2009; Shalev et al., 2013; Paytan et al., 2021) and MC–ICP–MS (Shalev et al., 2013), although MC–ICP–MS analytical protocols have tended to adopt standard-sample bracketing (SSB)–MC–ICP–MS (Fietzke and Eisenhauer, 2006; Moynier et al., 2010; Charlier et al., 2012; Ma et al., 2013). In general, DS–TIMS is considered to have the highest precision and accuracy, followed by DS–MC–ICP–MS and SSB–MC–ICP–MS.

Radiogenic and stable Sr isotopes were measured in this study using an MC–ICP–MS Neptune Plus instrument (Thermo Fisher Scientific, Germany). The mass bias was corrected using a combination of exponential law normalization ($^{87}Sr/^{86}Sr$ = 8.37861) and bracketing, with the normalized values being additionally corrected by the mean reference value of 0.710245 for SRM-987 strontium carbonate (GeoReM database, http://georem.mpch-mainz.gwdg.de/). To monitor the analytical procedure, SRM-987 was measured on a regular basis, yielding $^{87}Sr/^{86}Sr$ = 0.710261 ± 0.000020 (2SD, N = 257). The precision of the determinations estimated as the within-laboratory standard uncertainty (2σ) obtained for SRM-987 was ±0.003%. The precision of each individual result (1σ) during the sample measurement was better than ±20 ppm. Long-term analyses of $\delta^{88/86}Sr$ in SRM-987 processed through chromatographic columns and measured as unknowns yielded −0.01‰ ± 0.09‰ (2SD, N = 34). In addition, NIST SRM 1400 bone ash was analyzed as $\delta^{88/86}Sr$ = −0.33‰ ± 0.09‰ (2SD, N = 10), in agreement with the value provided in the GeoReM database. The precision of each individual result (1σ) was better than ±0.006‰.

3. Results

The studied samples are composed of limestone with a fine-grained matrix (micrite) containing abundant biogenic components (corals, coralline algae, molluscs, and benthic foraminifera) and undetermined carbonate fragments. Several samples contain fossil corals, including *Astrea* cf. *annuligera* Milne Edwards & Haime, 1849, *Porites* sp., and at least one other undetermined Merulinidae (Table 2 and Fig. 3). Large benthic foraminifera (LBF) represented by *Spiroclypeus tidoenganensis* Van der Vlerk, 1925 and *Heterostegina* cf. *assilinoides* (Blanckenhorn) Henson, 1937 occur in samples Lv86-9-6, Lv86-9-2, and Lv86-9-9 (sample numbers are given from oldest to youngest). Samples LV86-9 and LV86-16 consist of cidaroid echinoderm spines (identified by Dr. K.V. Minin, Shirshov Institute of Oceanology of Russian Academy of Sciences; Fig. 3B). The studied samples have a good degree of preservation, as assessed by optical examination.

In general, under the influence of post-sedimentary fluids, Fe and Mn contents increase and Sr and Mg decrease in carbonates (Veiser, 1983; Banner, 2004; Sawaki et al., 2010). Consequently, by studying the mutual correlations of these elements, it is possible to identify samples that have been least affected by diagenetic alteration. Samples with low Mn/Sr and Fe/Sr ratios are interpreted as not having undergone diagenetic processes, meaning that their isotope characteristics faithfully record those of the primary materials. The contents of Fe, Mn, Al, Sr, and Mg in our samples are very low, except in three samples (Table 3). The Fe/Sr ratio is particularly high in samples LV86-4 and LV86-8-2, with values of 0.74 and 0.77, respectively (Table 3). Sample LV86-8-2 also has a high Mn/Sr ratio (0.37), as does LV86-8-3 (0.60). These three samples (LV86-4, LV86-8-2, and LV86-8-3), for which at least one of the two ratios (Mn/Sr and Fe/Sr) is high, are used with caution in our interpretations, and the isotopic data derived from them are considered less reliable compared with other samples.

The Sr isotope compositions of two calcified echinoderm spines are very similar ($^{87}Sr/^{86}Sr$ = 0.70917 ± 0.000008, $\delta^{88/86}Sr$ 0.24 ± 0.01‰). Samples LV86-4, LV86-8-2, and LV86-8-3, which we infer to have undergone a degree of diagenetic alteration, have $^{87}Sr/^{86}Sr$ ratios of 0.708961, 0.708064, and 0.708000, respectively. The $^{87}Sr/^{86}Sr$ ratios of the remaining limestones range from 0.70817 to 0.70877, with a mean value of 0.70845 (Table 4), and their $\delta^{88/86}Sr$ values vary from 0.09‰ to 0.37‰, with a mean value of 0.22‰. An inverse relationship is observed between $\delta^{88/86}Sr$ and $^{87}Sr/^{86}Sr$ (correlation coefficient, $C_{cor} = -0.69$, $\rho = 0.13$), meaning that $\delta^{88/86}Sr$ decreases with decreasing Sr isotopic age. There is a positive relationship between isotopic composition and Sr content ($C_{cor} = 0.75$, $\rho = 0.08$). Here and below, the correlation coefficient is calculated as

$$Correl(X,Y) = \frac{\sum (x-\bar{x})(y-\bar{y})}{\sqrt{\sum (x-\bar{x})^2 \sum (y-\bar{y})^2}}$$

where $\bar{x}$ and $\bar{y}$ are mean values of two arrays.

4. Discussion

4.1. Sr isotope composition: $^{87}Sr/^{86}Sr$ and $\delta^{88/86}Sr$

The Sr isotope composition of seawater is recorded at the time of formation of carbonate skeletons of marine organisms (McArthur et al., 2001; Banner, 2004). The Sr isotope composition of ocean water results from the mixing of several Sr sources with different isotopic signatures (McArthur et al., 2001; Banner, 2004). Terrigenous material of continental origin with high $^{87}Sr/^{86}Sr$ ratios (modern value of continental runoff of 0.7116; Palmer and Edmond, 1989) is carried into ocean basins by rivers, glaciers, and wind. During the weathering of mid-ocean ridge basalts and halmyrolysis of ocean-floor rocks, Sr with a low $^{87}Sr/^{86}Sr$ ratio enters the water (modern value of 0.7037; Palmer and Edmond, 1989). The smallest sources of Sr are marine carbonates, which release upon recrystallization a part of the Sr held in the crystal lattice, which has an average isotopic ratio of 0.7084 (Holland, 1984; De Paolo, 1987; Davis et al., 2003; Banner, 2004). The modern global-ocean $^{87}Sr/^{86}Sr$ ratio is 0.70917 (Burke et al., 1982; Faure, 1986; Hodell et al., 1989; Banner, 2004; McArthur et al., 2012, 2020).

A comparison of the Sr isotope composition of carbonate rocks with the LOWESS global $^{87}Sr/^{86}Sr$ variation curve (McArthur et al., 2001, 2012, 2020) makes it possible to determine the age of their formation. The ratio of stable ^{88}Sr and ^{86}Sr isotopes (defined as $\delta^{88/86}Sr$ with respect to NIST SRM-987 or $\delta^{88/86}Sr$) in marine carbonates generally depends on the $\delta^{88/86}Sr$ value of seawater, which changes through time owing to variations in the same fluxes that control seawater $^{87/86}Sr$ and the net carbonate flux from the ocean, as well as the degree of fractionation between seawater and carbonate, which depends on species and temperature (Rüggeberg et al., 2008; Krabbenhöft et al., 2010; Vollstaedt et al., 2014; Pearce et al., 2015; Paytan et al., 2021). In the modern ocean, $\delta^{88/86}Sr$ is 0.378‰ to 0.402‰ (IAPSO standard seawater, http://georem.mpch-mainz.gwdg.de/sample_query.asp). Minerals such as carbonate formed in seawater are generally characterized by lower $\delta^{88/86}Sr$ than seawater because of seawater–mineral fractionation. Moreover, minerals of chemogenic and biogenic origins can be distinguished by the degree of their stable Sr isotope fractionation (Fietzke and Eisenhauer, 2006; Fruchter et al., 2016; AlKhatib and Eisenhauer, 2017; Müller et al., 2018), which depends on temperature and species. Thus, belemnites and cold-water corals do not exhibit temperature dependence of their stable Sr isotope fractionation (Rüggeberg et al., 2008; Vollstaedt et al., 2014), whereas $\delta^{88/86}Sr$ in tropical corals increases with sea surface temperature (Fietzke and Eisenhauer, 2006; Rüggeberg et al., 2008), and coccolithophores show an inverse temperature relationship (Stevenson et al., 2014). In our study of Koko Guyot, warm-water corals were replaced over time by deeper-water LBF and coralline algae In our study of Koko Guyot, warm-water corals were replaced over time by deeper-water LBF and coralline algae. Therefore, we expect that $\delta^{88/86}Sr$ will change over time in association with this species transition/replacement from warm/shallow to cold/deep types. However, in the present study, it is practically impossible to predict the direction of change (i.e., whether $\delta^{88/86}Sr$ will increase or decrease), due to there are many factors (including sea temperature, sea salinity, and skeleton/shell growth rates) that complicate the interpretation of $\delta^{88/86}Sr$ measurements.

Koko Guyot formed at *c.* 50 Ma (Jackson et al., 1980; Tarduno et al., 2003; Duncan and Keller, 2004), and this provides a key datum for the discussion below. The mean $^{87}Sr/^{86}Sr$ ratio of echinoid spines analyzed in this study is 0.70917 ± 0.00001, which corresponds to the modern isotopic water composition. Taking into account the errors associated with the LOWESS global $^{87}Sr/^{86}Sr$ variation curve (McArthur et al., 2001, 2012, 2020) we infer that the age of these echinoids is between 50 ka and the present (Fig. 4A). The youngest sample of unaltered limestones used for isotope stratigraphy is LV86-8-4, which yielded an age of 15.30 ± 0.15 Ma (Langhian, middle Miocene). Limestone sample LV86-9-1 was formed at 18.20 ± 0.15 Ma, and LV86-9-4 at 19.07 ± 0.03 Ma (Burdigalian, early Miocene). Sample LV86-9-9, which is composed of the remains of Merulinidae corals, formed at the Aquitanian–Burdigalian (early Miocene) boundary (20.1 ± 0.3 Ma), whereas the limestone sample LV86-9-2 containing *Astrea* cf. *annuligera* is Aquitanian in age (21.65 ± 0.3 Ma). The oldest studied sample, LV86-9-6, is Chattian (Oligocene) in age (25.55 ± 0.45 Ma). Samples LV86-9-2, LV86-9-6, and LV86-9-9, bearing *Spiroclypeus tidoenganensis* and *Heterostegina* cf. *assilinoides*, are latest Chattian (Oligocene) to Aquitanian in age. *Spiroclypeus tidoenganensis* has previously been recognized from the upper Oligocene of Koko Guyot (Hottinger, 1975). Although this species has been reported from coeval deposits in Saipan (Hanzawa, 1957), its Aquitanian age is firm (e.g., Hottinger, 1975; Lunt and Allan, 2007). The three limestone samples LV86-9-2, LV86-9-6, and LV86-9-9 have mean ages of 21.65, 25.55, and 20.10 Ma (based on Sr isotopes), respectively, consistent with the Chattian–Aquitanian age inferred from LBF species. A comparison with the LOWESS 3 global $^{87}Sr/^{86}Sr$ variation curve (McArthur et al., 2001, 2012) for altered samples LV86-4, LV86-8-2, and LV86-8-3 gives ages of 6.7 ± 0.3, 26.3 ± 0.5, and 29.2 ± 0.5 Ma, respectively. The last two ages are close to the age of LV86-9-6, suggesting that samples LV86-8-2 and LV86-8-3 may have approximately retained their initial compositions.

From 30 to 20 Ma, the $\delta^{88/86}Sr$ of seawater decreased from 0.38‰ to 0.30‰ (within ±0.02‰ analytical error) (Paytan et al., 2021; Fig. 4B). Five of the studied samples have ages within this time interval. Two of these samples (LV86-8-2 and LV86-8-3) have probably been affected by diagenetic alteration. Because diagenetic processes have been shown to alter the initial $\delta^{88/86}Sr$ of carbonates (Voigt et al., 2015), we use only the three least modified samples as a basis for our discussion. The $\delta^{88/86}Sr$ value of these samples varies from 0.26‰ to 0.37‰. Within the margin of error (±0.09‰), the results obtained intersect the line indicating the isotopic composition of seawater proposed by Paytan et al. (2021). The stable Sr isotope composition of younger samples from 20 to 15 Ma (LV86-8-4, LV86-9-1, and LV86-9-4) comprising cold-water sea species and lacking corals is rather uniform, with the mean $\delta^{88/86}Sr$ varying within 0.10‰ ± 0.03‰. These values are much lower than the isotope curve proposed by Paytan et al. (2021) (Fig. 4B). The $\delta^{88/86}Sr$ values of modern echinoids are also lower than (although within measurement errors of) the $\delta^{88/86}Sr$ curve.

It has been shown that carbonates have lower $\delta^{88/86}$ Sr values than the sedimentation medium, and the difference can be more than 0.1‰ (Raddatz et al., 2013, Vollstaedt et al., 2014). Kisakürek et al. (2011) and Böhm et al. (2013) explained this disparity by calcification in a largely open system at high precipitation rates. The shift to a benthic community that is more resistant to colder water can be correlated with bottom subsidence and guyot migration to higher latitudes (Wilson, 1963; Clague and Dalrymple, 1987; Tarduno et al., 2003; Clague et al., 2010). The change in temperature and light regime at Koko Guyot as it subsided and migrated to higher latitudes led to a change in the benthic community as reef benthic assemblages were replaced by those dominated by LBF (and coralline algae). The change in temperature and light regime at

Koko Guyot as it subsided and migrated to higher latitudes led to a change in the benthic community as reef assemblages were replaced by those dominated by LBF and coralline algae. We presume that this change in benthic community is recorded as a sharp decrease in $\delta^{88/86}$Sr valuesi in our samples compared to sea water (Fig. 4B) without major changes in seawater $\delta^{88/86}$Sr values It is probable that Sr isotope fractionation between cold-water species and ambient seawater is much stronger than that between warm-water species and ambient seawater. However, we cannot take into account temperature and depth changes in this paper.

4.2. Rate of subsidence of Koko Guyot and its variation over time

Grigg (1988) identified corals *Favites* sp., *Platygyra* sp., *Psammocora (Stephanaria*) sp., and *Seriatopora* sp. from Koko Seamount, the ages of which ranged from 30.5 to 24.7 Ma, as determined using Sr isotope stratigraphy. Clague et al. (2010) obtained ages for corals ranging from 50 to 27 Ma, compared with 16 Ma for LBF, on the basis of which those authors calculated the subsidence rate of the volcano as 0.012 ± 0.003 mm/yr. Davies et al. (1972) used water depth, guyot structure, and the age and species composition of corals to estimate the subsidence rate of Koko Guyot as 0.042 mm/yr throughout the existence of the guyot.

Our method of estimation of subsidence rates for Koko Guyot incorporated the following assumptions: (1) reef formation slowed and then stopped owing to submersion below the euphotic zone, which is the lower depth limit of coral and algal growth; (2) the identified fossil benthic assemblage from the guyot plateau lived in optimal depth (i.e., 0–30 m) and temperature (average winter water temperature >18 °C) conditions for reef growth (Veron, 1995); and (3) later benthic communities, devoid of reef corals, lived at greater water depths >30 m. Warm-water corals grow at a certain depth, no more than 30 m (Veron, 1995). As the seafloor subsides and relative sea-level rise resultantly occurs, the reef builds up vertically to retain a zone of maximum favorability for coral existence. We took the maximum water depth of this zone for corals in this study as 30 m. We also assumed that the formation of the carbonate skeleton occurred under normal conditions. With gradual subsidence of the seafloor, we assumed that the reef of Koko Guyot was able to keep up with sea-level rise so long as the seafloor was within the euphotic zone. As the rate of sinking increased, new colonies would have formed more quickly to grow to a favorable depth (maximum 30 m). With a high subsidence rate, the coral growth rate will also be faster. The «new» corals will record the «new» isotopic composition of water. Thus, samples with a small difference in age will occur more often. Thus, we have described our «model object» and proceed to the calculations.

We took all age estimates (Grigg, 1988; Clague et al., 2010; this work), ranked them from youngest to oldest, and calculated the difference between each successive age (which ranged from 0 to 2 Myr), thus obtaining 26 datapoints (Table 5 and Fig. 5). Figure 5 shows that the age difference between the samples during the early stage of guyot evolution is small and that this difference increases with Koko Guyot age. The pattern of data in Fig. 5 suggests that the rate of reef growth (or of the guyot's subsidence) varied over time. The age difference for the period 30–25 Ma is smaller than that for 25–15 Ma, suggesting that the reef grew more quickly during the older period. The age of the youngest identified coral specimen is 20.1 ± 0.3 Ma (LV86-9-9). This sample may therefore mark the final episode of active reef growth, after which the platform deepened to a position below the euphotic zone (Wilson, 1963; Clague and Dalrymple, 1987; Tarduno et al., 2003; Clague et al., 2010). We also sampled a coralline algal crust dated at 15 Ma (LV86-8-4). The sample was collected from a depth of 1458 m, where it was located in a soft (unconsolidated) substrate. This sample most likely slid down the slope from the nearest plateau, whose current top height is at 350 m water depth. Assuming a maximum water depth of 120 m for the living coralline algae and 30 m for the living youngest zooxanthellate corals sampled (Clague et al., 2010), we calculated the following: (1) From 15 Ma to the present, Koko Guyot subsided at a rate of (350 − 120)/15.3 = 15.0 m/Myr, that is, 0.015 ± 0.002 mm/yr; and (2) during the period from 20 to 15 Ma, the mean subsidence rate was (120 − 30)/(20.1 − 15.3) = 18.8 m/Myr, that is, 0.019 ± 0.003 mm/yr. A previous study has suggested that the initial shallow-water sediments formed during the period from 49.7 to 43.5 Ma, as identified in the ODP Site 1206 (Fig. 1) core recovered at 1500 m water depth (Shipboard Scientific Party, 2002). The bottom of this layer was 57 m from the top of the column (Shipboard Scientific Party, 2002; Tarduno et al., 2003). Thus, applying our calculation method, the subsidence rate during the first tens of million years (from 49.7 to 43.5 Ma) is estimated as 0.046 ± 0.005 mm/yr [using (1500 + 57 − 350)/(46.6 − 20.1) = 46.2 m/Myr or 0.046 ± 0.005 mm/yr, where 46.6 Ma is the mean of 49.7 and 43.5 Ma] (Fig. 6), which is close to the rate reported by Davies et al. (1972). Our calculated average subsidence rate is higher than that estimated by Clague et al. (2010) of 0.008–0.012 mm/yr since 23 Ma. However, our results are consistent with the observation that the subsidence rate of the ocean floor decreases as the age of the ocean crust increases (e.g., Sclater et al., 1980; Marty and Cazenave, 1989; Stein and Stein, 1992). This process represents seafloor flattening, meaning that old seafloor is shallower than that predicted by the "root-t" model (i.e., a linear increase in ocean depth with increasing crustal age; Parsons and Sclater, 1977; Hillier, 2010).

5. Conclusions

We investigated the Sr isotope compositions of Oligocene–Miocene coral reef limestone from Koko Guyot in the southern Emperor Seamount Chain to assess the dynamics of the subsidence of this guyot. Our study of Sr isotope compositions ($^{87}Sr/^{86}Sr$) showed that the least altered limestones containing fragments of reef corals were formed during the early Miocene. No coral fragments were found in older samples (late Oligocene). Analysis of the distribution of stable Sr isotopes ($\delta^{88/86}Sr$) in warm-water sediments showed a low degree of fractionation compared with seawater. The $\delta^{88/86}Sr$ values of cold-water species, which replaced warm-water species at around 20 Ma, differ significantly from the seawater $\delta^{88/86}Sr$ variation curve estimated by Paytan et al. (2021).

Using several independent methods, we confirmed a change in environmental parameters at around 20 Ma. This timing also corresponds to a change in the rate of subsidence. From 49–44 to 20 Ma, the subsidence rate of Koko Guyot was 0.046 ± 0.005 mm/yr. The $\delta^{88/86}Sr$ values of coral samples that formed from 25 to 20 Ma vary from 0.26‰ to 0.37‰ (±0.09‰) and are consistent with the variation curve proposed by Paytan et al. (2021). At the ending of this period, the benthic community changed because of cooling ambient waters. Warm-water corals disappeared and were replaced by LBF and coralline algae. From 20 to 15 Ma, the subsidence rate was much lower at 0.019 ± 0.003 mm/yr. The $\delta^{88/86}Sr$ values for samples that formed during this period are ~0.10‰. Since 15 Ma, the volcanic structure has subsided at a rate of 0.015 ± 0.002 mm/yr. The data obtained in this study refine existing models of the crustal subsidence of the floor of the Pacific Ocean, which suggest a constant rate of seafloor subsidence. Understanding the changing rate of subsidence is important because it is related to the process of ocean-floor cooling after the Pacific Plate passed over the mantle Hawaiian hotspot.

Declaration of competing interests

The authors declare that they have no known competing financial interests or personal relationships that could have appeared to influence the work reported in this paper.

Acknowledgments

The authors are grateful to Tatyana Nikolaevna Dautova (Head of the 86th voyage of the research vessel “Akademik M.A. Lavrentiev”) and to A.V. Zhirmunsky (National Scientific Centre of Marine Biology, Far Eastern Branch, Russian Academy of Sciences Vladivostok) for organizing the work; and to the members of the Deepwater Equipment Department of A.V.

Zhirmunsky National Scientific Centre of Marine Biology, Far Eastern Branch, Russian Academy of Sciences (NSCMB FEB RAS) and Alexei Mikhailovich Asavin for their help with rock sampling. The authors thank Aleksey Kotov for his assistance with carbonate rock sample analyses.

We thank Editor-in-Chief of Marine Geology Dr. Adina Paytan and anonymous reviewers for their valuable comments and suggestions, which improved the quality of the manuscript.

Participation in the 86th voyage of the R/V “Akademik M.A. Lavrentiev” was made possible owing to a state assignment of the FEGI FEB RAS (state registration number AAAA-A17-117092750071-2). The reequipment and comprehensive development of the “Geoanalitik” shared research facilities of the IGG UB RAS was financially supported by a grant by the Ministry of Science and Higher Education of the Russian Federation for 2021–2023 (Agreement No. 075-15-2021-680). Chemical and isotopic investigations were conducted in the Geoanalitik Center for Collective Use of the IGG UB RAS as part of the state assignments of the GEOCHI RAS and IGG UB RAS (state registration number AAAA-A18-118053090045-8).

Data availability

All data are provided in attached files and at https://doi.org/10.5281/zenodo.6330970.

References

AlKhatib, M., Eisenhauer, A., 2017. Calcium and strontium isotope fractionation during precipitation from aqueous solutions as a function of temperature and reaction rate; II. Aragonite. Geochim. Cosmochim. Acta, 209, 320-342. https://doi.org/10.1016/j.gca.2017.04.012

Banner, J.L., 2004. Radiogenic isotopes: systematics and applications to earth surface processes and chemical stratigraphy. Earth-Sci. Rev. 65, 141–194. https://doi.org/10.1016/S0012-8252(03)00086-2

Böhm, F., Eisenhauer, A., Tang, J., Dietzel, M., Krabbenhöft, A., Kisakürek, B., Horn, C. 2012. Strontium isotope fractionation of planktic foraminifera and inorganic calcite. Geochim. Cosmochim. Acta, 93, 300-314. https://doi.org/10.1016/j.gca.2012.04.038

Burke, W.H., Denison, R.E., Hetherington, E.A., Koepnick, R.B., Nelson, H.F., Otto, J.B., 1982. Variation of seawater $^{87}Sr/^{86}Sr$ throughout Phanerozoic time. Geology 10, 516–519.

Certificate of analysis IAG / CGL 020 ML-3 (Limestone), 2015. International Association of Geoanalysts http://iageo.com/wp-content/uploads/2020/08/ML-3-certificate.pdf (accept 17.07.2022)

Charlier, B.L.A., Nowell, G.M., Parkinson, I.J., Kelley, S.P., Pearson, D.G., Burton, K.W., 2012. High temperature strontium stable isotope behaviour in the early solar system and planetary bodies. Earth Planet Sci Lett 329, 31–40.

Clague, D.A., Braga, J.C., Bassi, D., Fullagar, P.D., Renema, W., Webster, J.M., 2010. The maximum age of Hawaiian terrestrial lineages: geological constraints from Kōko Seamount. J. Biogeogr. 37, 1022–1033. https://doi.org/10.1111/j.1365-2699.2009.02235.x

Clague, D.A., Dalrymple, G.B., 1987. The Hawaiian-Emperor volcanic chain. part I. Geologic evolution. Volcanism in Hawaii. 1, 5–54.

Dalrymple, G.B., Clague, D.A., 1976. Age of the Hawaiian–Emperor bend. Earth Plan. Sci. Lett. 31, 313–329.

Davies, T.A., Wilde, P., Clague, D.A., 1972. Koko Seamount: A major guyot at the southern end of the Emperor Seamounts. Mar. Geol. 13, 311–321.

Davis, A.C., Bickle, M.J., Teagle, D.A.H. Imbalance in the oceanic strontium budget. Earth Planet. Sci. Lett., 2003. 211, 173– 187.

DePaolo, D.J., 1987. Correlating rocks with strontium isotopes. Geotimes 32 (12), 16–18.

Duncan, R.A., Keller, R.A., 2004. Radiometric ages for basement rocks from the Emperor Seamounts, ODP Leg 197. Geochem. Geophys. Geosyst., 5, Q08L03. doi:10.1029/2004GC000704

Faure, G., 1986. Principles of Isotope Geology. 2nd ed. New York, Willey et Sons.

Fietzke, J., Eisenhauer, A., 2006. Determination of temperature-dependent stable strontium isotope ($^{88}Sr/^{86}Sr$) fractionation via bracketing standard MC-ICP-MS. Geochem. Geophys. Geosyst. 7, Q08009, doi:10.1029/2006GC001243

Fruchter, N., Eisenhauer, A., Dietzel, M., Fietzke, J., Böhm, F., Montagna, P., Stein, M., Lazar, B., Rodolfo-Metalpa, R., Erez, J., 2016. 88Sr/86Sr fractionation in inorganic aragonite and in corals. Geochimica et Cosmochimica Acta 178, 268-280, https://doi.org/10.1016/j.gca.2016.01.039

GeoReM database http://georem.mpch-mainz.gwdg.de/ (accept 17.07.2022)

Greene, H.G., Clague, D.A., Dalrymple, G.B., 1980. Seismic stratigraphy and vertical tectonics of the Emperor Seamounts. DSDP Leg 55. Initial reports of the Deep Sea Drilling Project. Wash. (D.C.), US Gov. print, off. 55, 759–788.

Grigg, R.W., 1988. Paleoceanography of coral reefs in the Hawaiian-Emperor Chain. Science 240, 1737–1743.

Hanzawa, S. 1957. Cenozoic foraminifera of Micronesia. Geol. Soc. Am., Mem. 66, 163 pp.

Henson, F.R.S., 1937. Larger foraminifera from Aintab, Turkish Syria. Eclog. Geol. Helv. 30, 45-57.

Hillier, J.K., 2010. Subsidence of "normal" seafloor: Observations do indicate "flattening". J. Geophys. Res. Solid Earth 115(B3). https://doi.org/10.1029/2008JB005994

Hodell, D.A., Mueller, P.A., McKenzie, J.A., Mead, G.A., 1989. Strontium isotope stratigraphy and geochemistry of the late Neogene ocean. Earth Planet. Sci. Lett. 92, 165–178.

Holland, H.D., 1984, The Chemical Evolution of the Atmosphere and Oceans. Princeton University Press, Princeton, NJ, pp. 582.

Hottinger, L. 1975. Late Oligocene larger foraminifera from Koko Guyot, site 309. Initial Reports of the Deep Sea Drilling Project, 32, 825–826.

Jackson, E. D., Koisumi, I., Dalrymple, G., Clague, D., Kirkpatrick, R., Greene, H., 1980. Introduction and summary of results from DSDP Leg 55, the Hawaiian–Emperor hot-spot experiment. Initial reports of the deep sea drilling project, 55, 5–31.

Jochum, K.P., Garbe-Schonberg, D., Veter, M., Stoll, B., Weis, U., Weber, M., Lugli, F., Jentzen, A., Schiebel, R., Wassenburg, J.A., Jacob, D.E., Haug, G.H., 2019. Nano-powdered calcium carbonate reference materials: significant progress for microanalysis? Geostand. Geoanal. Res. 43: 595-609. https://doi.org/10.1111/ggr.12292

Keller, R.A., Fisk, M.R., White, W.M., 2000. Isotopic evidence for Late Cretaceous plume–ridge interaction at the Hawaiian hotspot. Nature 405(6787), 673–676. doi:10.1038/35015057

Kisakürek, B., Eisenhauer, A., Böhm, F., Hathorne, E.C., Erez, J., 2011. Controls on calcium isotope fractionation in cultured planktic foraminifera, *Globigerinoides ruber* and *Globigerinella siphonifera*. Geochim. Cosmochim. Acta, 75, 427-443. https://doi.org/10.1016/j.gca.2010.10.015

Krabbenhöft, A., Eisenhauer, A., Böhm, F., Vollstaedt, H., Fietzke, J., Liebetrau, V., Augustin, N., Peucker-Ehrenbrink, B., Müller, M.N., Horn, C., Hansen, B.T., Nolte, N., Wallmann, K., 2010. Constraining the marine strontium budget with natural strontium isotope fractionations (^{87}Sr/^{86}Sr∗, $\delta^{88/86}$Sr) of carbonates, hydrothermal solutions and river waters. Geochim. Cosmochim. Acta 74 (14), 4097-4109. https://doi.org/10.1016/j.gca.2010.04.009

Krabbenhoft, A., Fietzke, J., Eisenhauer, A., Liebetrau, V., Bohm, F., Vollstaedt, H., 2009. Determination of radiogenic and stable strontium isotope ratios (^{87}Sr/^{86}Sr, $\delta^{88/86}$Sr) by thermal ionization mass spectrometry applying an ^{87}Sr/^{84}Sr double spike. J Anal At Spectrom 24, 1267–1271

Kuznetsov, A.B., Gorokhov, I.M., Semikhatov, M.A., 2018. Strontium isotope stratigraphy: Principles and State of the Art. Strat. Geol. Correl. 26, 367–386. https://doi.org/10.1134/S0869593818040056

Larson, R.L., Moberly, R., Bukry, D., Foreman, H.P., Gardner, J.V., Keene, J.B., Lancelot, Y., Luterbacher, H., Marshall, M.C., Matter, A., 1975. Site 308: Koko guyot. Site 309: Koko guyot. Initial reports of the Deep Sea Drilling Project. Wash. (D.C.): US Gov. print, off. 32, 215–231.

Lunt, P., Allan, T. 2004. Larger foraminifera in Indonesian biostratigraphy, calibrated to isotopic dating. Geological Research Development Centre Museum, Workshop on Micropalaeontology, Bandung, 109 pp.

Ma, J.L., Wei, G.J., Liu, Y., Ren, Z.Y., Xu, Y.G., Yang, Y.H., 2013. Precise measurement of stable ($\delta^{88/86}Sr$) and radiogenic ($^{87}Sr/^{86}Sr$) strontium isotope ratios in geological standard reference materials using MC-ICP-MS. Chinese Science Bulletin 58, 3111–3118.

Marty, J.C., Cazenave, A., 1989. Regional variations in subsidence rate of oceanic plates: a global analysis. Earth Plan. Sci. Let., 94 (3–4), 301-315, https://doi.org/10.1016/0012-821X(89)90148-9

McArthur, J.M., Howarth, R.J., Shields, G.A., 2012. Strontium isotope stratigraphy. The Geologic Time Scale 1, 127–144. DOI: 10.1016/B978-0-444-59425-9.00007-X

McArthur, J.M., Howarth, R.J., Shields, G.A., Zhou, Y., 2020. Chapter 7. Strontium Isotope Stratigraphy, in Gradstein, F.M., Ogg, J.G., Schmitz, M.D., Ogg, G.M. (Eds), Geologic Time Scale 2020, Elsevier, pp. 211–238, https://doi.org/10.1016/B978-0-12-824360-2.00007-3

McArthur, M., Howaith, R.J., Bailey, T.R., 2001. Strontium isotope stratigraphy: LOWESS Version 3: Best Fit to the Marine Sr-Isotope Curve for 0-509 Ma and Accompanying Look-up Table for Deriving Numerical Age. J. Geol. 109, 155–170. https://doi.org/10.1086/319243

Moynier, F., Agranier, A., Hezel, D.C., Bouvier, A., 2010. Sr stable isotope composition of Earth, the Moon, Mars, Vesta and meteorites. Earth Planet Sci Lett 300, 359–366

Milne Edwards, H., Haime, J., 1848. Recherches sur les polypiers. Mémoire 4. Monographie des Astréides (1) (suite). Annales des Sciences Naturelles, Zoologie, Series 3. 12, 3, 95-197.

Müller, M.N., Krabbenhöft, A., Vollstaedt., H, Brandini, F.P., Eisenhauer, A., 2018. Stable isotope fractionation of strontium in coccolithophore calcite: Influence of temperature and carbonate chemistry. Geobiology, 16, 297– 306. https://doi.org/10.1111/gbi.12276

Palmer, M.R., 1985. Rare earth elements in foraminifera tests. Earth Planet. Sci. Lett. 73(2-4), 285–298. doi:10.1016/0012-821x(85)90077-9

Palmer, M.R., Edmond, J.M., 1989. The strontium isotope budget of the modern ocean // Earth Planet. Sci. Letters 92, № 61, 11-26

Parsons, B., Sclater, J. G., 1977. An analysis of the variation of ocean floor bathymetry and heat flow with age. J. Geophys. Res. 82(5), 803–827.

Paytan, A., Griffith, E.M., Eisenhauer, A., Hain, M.P., Wallmann, K., Ridgwell, A., 2021. A 35-million-year record of seawater stable Sr isotopes reveals a fluctuating global carbon cycle. Science 371 (6536), 1346–1350. DOI: 10.1126/science.aaz9266

Pearce, C.R., Parkinson, I.J., Gaillardet, J., Charlier, B.L.A., Mokadem, F., Burton, K.W., 2015. Reassessing the stable ($\delta^{88/86}$Sr) and radiogenic (^{87}Sr/^{86}Sr) strontium isotopic composition of marine inputs. Geochim. Cosmochim. Acta 157, 125–146. https://doi.org/10.1016/j.gca.2015.02.029

Raddatz, J., Liebetrau, V., Rüggeberg, A., Hathorne, E., Krabbenhöft, A., Eisenhauer, A., Böhm, F., Vollstaedt, H., Fietzke, J., López Correa, M., Freiwald, A., Dullo, W.-Chr., 2013. Stable Sr-isotope, Sr/Ca, Mg/Ca, Li/Ca and Mg/Li ratios in the scleractinian cold-water coral Lophelia pertusa. Chem. Geol., 352, 143-152. https://doi.org/10.1016/j.chemgeo.2013.06.013

Rüggeberg, A., Fietzke, J., Liebetrau, V., Eisenhauer, A., Dullo, W.-C., Freiwald, A., 2008. Stable strontium isotopes ($\delta^{88/86}$Sr) in cold-water corals — A new proxy for reconstruction of intermediate ocean water temperatures. Earth Planet. Sci. Lett. 269 (3–4), 570–575. https://doi.org/10.1016/j.epsl.2008.03.002

Sawaki, Y., Ohno, T., Tahata, M., Komiya, T., Hirata, T., Maruyama, S., Windley, B.F., Han, J., Shu, D., Li, Y., 2010. The Ediacaran radiogenic Sr isotope excursion in the Doushantuo Formation in the Three Gorges area, South China. Precambrian Res. 176, 46–64. https://doi.org/10.1016/j.precamres.2009.10.006

Sclater, J. G., Jaupart, C., Galson, D., 1980. The heat flow through oceanic and continental crust and the heat loss of the Earth. Rev. Geoph. Space Physics, 18 (1), 269-311 https://doi.org/10.1029/RG018i001p00269

Shalev, N., Segal, I., Lazar, B., Gavrieli, I., Fietzke, J., Eisenhauer, A., Halicz, L., 2013. Precise determination of δ88/86Sr in natural samples by double-spike MC-ICP-MS and its TIMS verification. J Anal At Spectrom 28, 940–944.

Shipboard Scientific Party, 1975a. Site 308: Koko Seamount. Proceedings of the Deep Sea Drilling Project, Initial Reports, Vol. 32 (by R.L. Larson, R. Moberly, D. Bukry, H.P. Foreman, J.V. Gardner, J.B. Keene, Y. Lancelot, H. Luterbacher, M.C. Marshall and A. Matter), pp. 215–226. US Government Printing Office, Washington, DC.

Shipboard Scientific Party, 1975b. Site 309: Koko Seamount. Proceedings of the Deep Sea Drilling Project, Initial Reports, Vol. 32 (by R.L. Larson, R. Moberly, D. Bukry, H.P. Foreman, J.V. Gardner, J.B. Keene, Y. Lancelot, H. Luterbacher, M.C. Marshall and A. Matter), pp. 227–231. US Government Printing Office, Washington, DC.

Shipboard Scientific Party, 2002. Site 1206. Proceedings of the Ocean Drilling Program, Initial Reports, Vol. 197 (by J.A. Tarduno, R.A. Duncan and D.W. Scholl et al.), pp. 1–117. Ocean Drilling Program, College Station, TX.

Speijer, R. P., Pälike, H., Hollis, C. J., Hooker, J. J., Ogg, J. G., 2020. The Paleogene Period. In Geologic time scale 2020, 1087-1140. Elsevier.

Stein, C., Stein, S., 1992. A model for the global variation in oceanic depth and heat flow with lithospheric age. Nature 359, 123–129. https://doi.org/10.1038/359123a0

Stevenson, E.I., Hermoso, M., Rickaby, R.E.M., Tyler, J.J., Minoletti, F., Parkinson, I.J., Mokadem, F., Burton, K.W., 2014. Controls on stable strontium isotope fractionation in coccolithophores with implications for the marine Sr cycle. Geochim. Cosmochim. Acta 128, 225–235. https://doi.org/10.1016/j.gca.2013.11.043

Stoll H.M., Schrag D.P., 1998. Effects of Quaternary sea level cycles on strontium in seawater. Geochim. Cosmochim. Acta 62, 1107–1118. doi:10.1016/S0016-7037(98)00042-8

Tarduno, J.A., Duncan, R.A., Scholl, D.W., Cottrell, R.D., Steinberger, B., Thordarson, Th., Kerr, B.C., Neal, C.R., Frey, F.A., Torii, M., Carvallo, C., 2003. The Emperor Seamounts: southward motion of the Hawaiian Hotspot Plume in Earth's mantle. Science 301, 1064–1069. doi: 10.1126/science.1086442

Teng, F.-Z., Dauphas, N., Watkins, J.M., 2017. Non-Traditional Stable Isotopes: Retrospective and Prospective. Reviews in Mineralogy and Geochemistry 82(1), 1–26. doi: https://doi.org/10.2138/rmg.2017.82.1

Van der Vlerk, M., 1925. A study of Tertiary foraminifera from the "Tidoengsche Landen" (E Borneo). Nederl. Indie, Dienst Mijnb. Wetensch. Meded. 3, 13-38.

Veiser, J., 1983. Trace elements and isotopes in sedimentary carbonate. Carbonates: mineralogy and chemistry. Rev. Min. 11 (2), 260–299.

Veron, J.E.N., 1995. Corals in space and time: the biogeography and evolution of the Scleractinia. UNSW Press, Sydney NSW Australia, 321 pp.

Vishnevskaya, I.A., Okuneva, T.G., Kiseleva, D.V., Soloshenko, N.G., Streletskaya, M.V., Vosel, Yu.S., 2020. Trace element and Sr isotopic composition of bottom and near-surface oceanic water in the southern region of the Emperor Ridge. Mar. Chem. 224, 103808. https://doi.org/10.1016/j.marchem.2020.103808

Voigt, J., Hathorne, Ed C., Frank, M., Vollstaedt, H., Eisenhauer, A., 2015. Variability of carbonate diagenesis in equatorial Pacific sediments deduced from radiogenic and stable Sr isotopes. Geochim. Cosmochim. Acta 148, 360–377, http://dx.doi.org/10.1016/j.gca.2014.10.001

Vollstaedt H., Eisenhauer A., Wallmann K., Böhm F., Fietzke J., Liebetrau V., Krabbenhöft A., Farkaš J., Tomašových A., Raddatz J., Veizer J., 2014. The Phanerozoic δ88/86Sr record of seawater: New constraints on past changes in oceanic carbonate fluxes. Geochim. Cosmochim. Acta 128, 249–265, https://doi.org/10.1016/j.gca.2013.10.006

Wheeler, C.W., Aharon, P., 1991. Mid-oceanic carbonate platforms as oceanic dipsticks: examples from the Pacific. Coral Reefs 10, 101–114.

Wilson, J.T., 1963. A possible origin of the Hawaiian Islands. Canadian J. Phys. 41, 863–870.

Figure and table captions

Fig. 1. (A) Geographic map of the Hawaiian–Emperor bend. (B) Bathymetric map of Koko Guyot. Points represent sampling sites for dives 4, 8, 9, and 16. Deep Sea Drilling Project sites 308 and 309 and Ocean Drilling Program Site 1206 are shown by value. The source of the bathymetric map is http://earthref.org.

Fig. 2. Photographs of sampling conducted by a Comanche remotely operated underwater vehicle. (A) Rock sampling from the plateau of the guyot using a manipulator (dive 9; sample Lv86-9-2); (B) Sampling using a scoop net mounted on the manipulator (dive 9; sample Lv86-9 echinoid).

Fig. 3. (A) Modern octocoral of the Isididae family (sample Coral). (B) Echinoderm spines (Cidaroida; sample LV86-9, echinoid). (C–D) Larger-foraminiferal packstone with *Spiroclypeus tidoenganensis* (*St*) and *Heterostegina* cf. *assilinoides* (*Ha*) (samples Lv86-9-2 and Lv86-9-6). (E) Reef coral *Astrea* cf. *annuligera* (sample Lv86-9-2; i, thickened costo-septum; ii, paliform lobe). (F–G) Bioclastic packstone showing (F) the encrusting coralline *Lithoporella* sp. with two uniporate conceptacles (arrows; sample LV86-8-3; conc., conceptacle) and (G) bryozoans (bry) and coralline fragments (cor; sample LV86-9-4).

Fig. 4. Comparison of the Sr isotopic composition of the studied samples with (A) the radiogenic Sr isotope record (LOWESS 3; McArthur et al., 2001) and (B) a model of the stable Sr isotope

record with ±0.02‰ analytical uncertainty (gray area; Paytan et al., 2021) in the ocean. Crossed-out circles represent data from diagenetically altered samples. Error bars are ±0.09‰.

Fig. 5. Relationship between age and age difference between two consecutive ages for carbonate samples. The difference between the ages of consecutive older samples is less than that of the younger samples. This suggests that the rate of subsidence of the reef superstructure was initially high and subsequently decreased (i.e., the subsidence rate was higher when the coral reef and the guyot were younger). Data from this work (circles), Grigg (1988, diamonds), and Clague et al. (2010, squares) are plotted in the figure.

Fig. 6. Schematic model for the vertical motion of Koko Guyot. The bold line in the graph shows the changing position of the summit of the volcano, which formed at 49–48 Ma (Jackson et al., 1980; Tarduno et al., 2003; Duncan and Keller, 2004). The rates given in the figure indicate the subsidence rate, calculated using the method presented in Section 4.2.

Table 1. Coordinates and depth of samples analysed in this study, and seawater temperature and salinity at the sampling sites.

T, water temperature; S, salinity; Coral, sample of modern isididae coral; echinoid, sample of echinoid spines

Table 2. Lithology and biotic components from the studied Koko Guyot carbonate samples.

Table 3. Trace-element contents and calculated Fe/Sr and Mn/Sr ratios of the studied carbonates. Analyses were performed using ICP–AES. Contents are given in ppm.

Table 4. Strontium isotope compositions and ages according to LOWESS 3 (McArthur et al., 2001, 2012).

Table 5. Strontium isotope ages of samples from the present study and previous studies (blue, Grigg, 1988; yellow, Tarduno et al., 2003; green, Clague et al., 2010; white, this study) used to calculate age differences between consecutive samples.

Figure 1

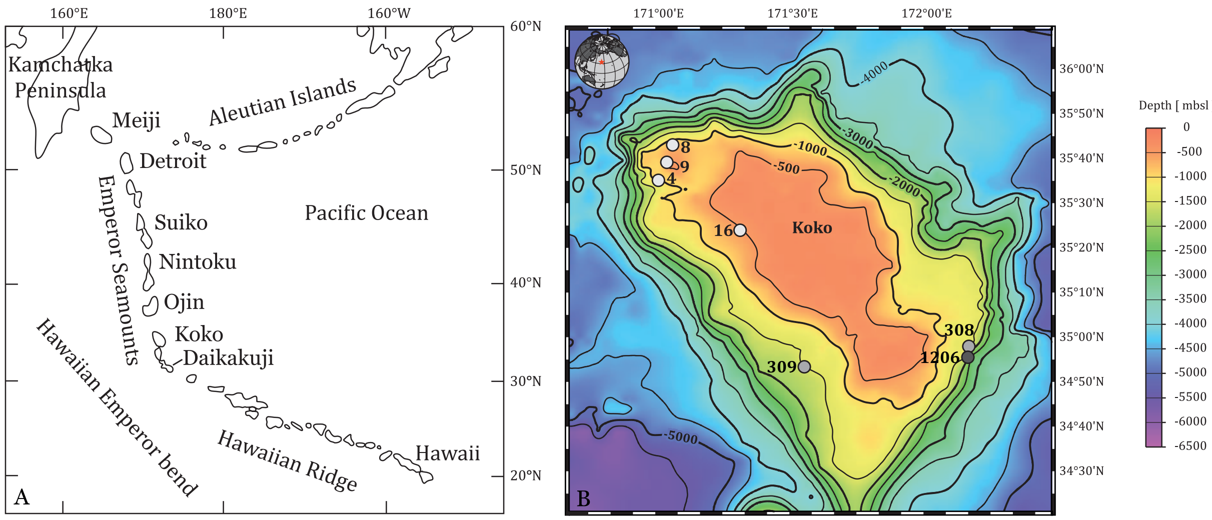
160°E
180°E
160°W
60°N
50°N
40°N
30°N
20°N
Kamchatka
Peninsula
Meiji
Aleutian Islands
Detroit
Emperor Seamounts
Suiko
Pacific Ocean
Nintoku
Ojin
Koko
Daikakuji
Hawaiian Emperor bend
Hawaiian Ridge
Hawaii
A
171°00'E
171°30'E
172°00'E
36°00'N
35°50'N
35°40'N
35°30'N
35°20'N
35°10'N
35°00'N
34°50'N
34°40'N
34°30'N
-4000
-3000
-1000
-500
-2000
-5000
8
9
4
16
Koko
308
1206
309
B
Depth [mbsl]
0
-500
-1000
-1500
-2000
-2500
-3000
-3500
-4000
-4500
-5000
-5500
-6000
-6500

Figure 2

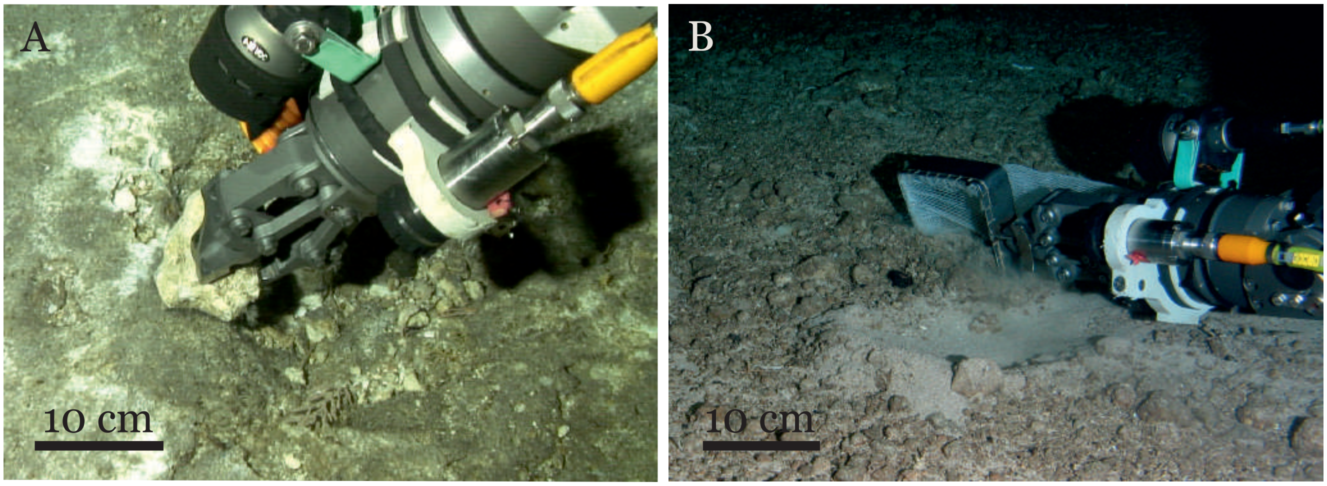

Figure 3

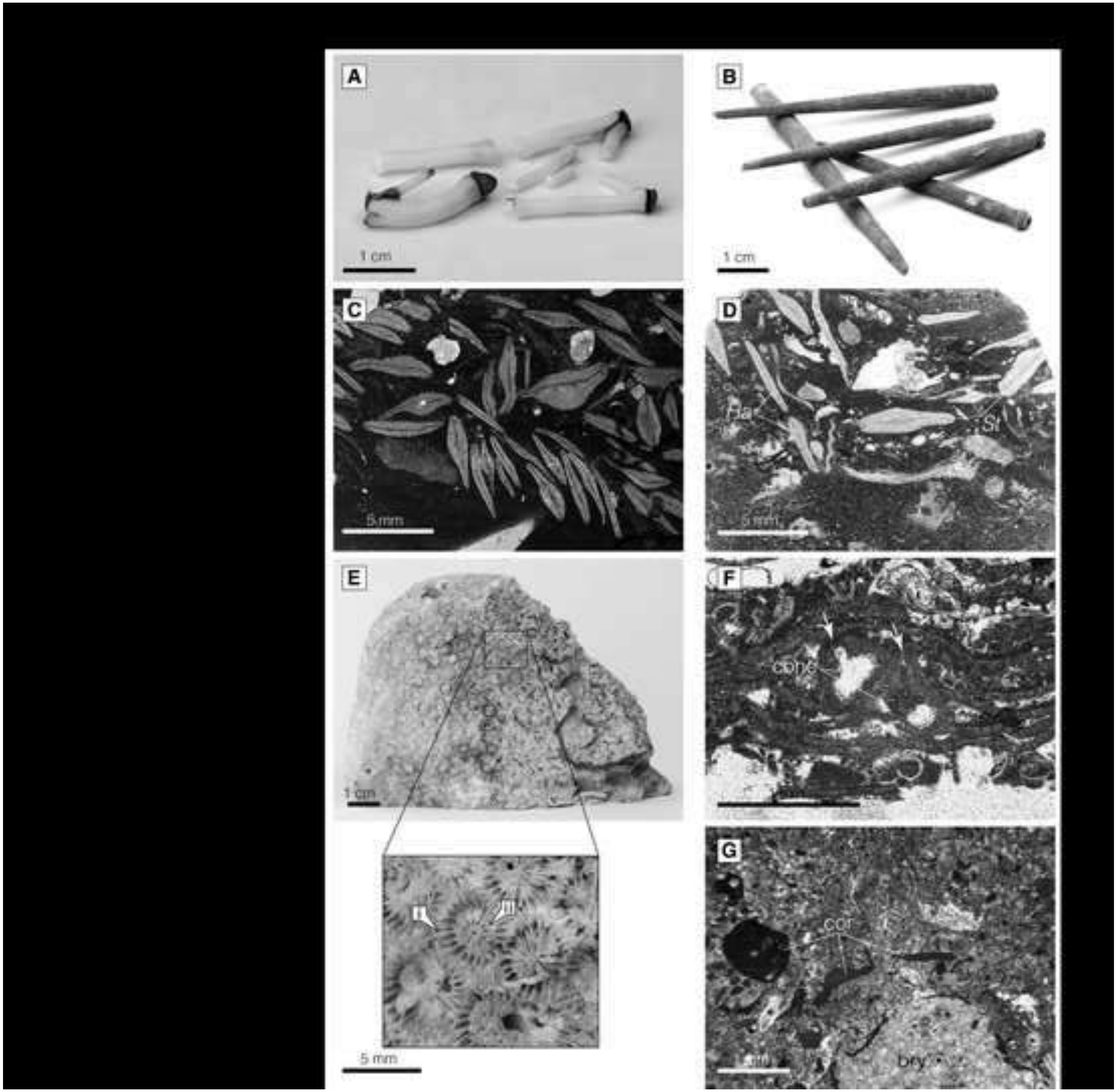

Figure 4

Click here to access/download;Figure;Fig 4 Sr-Sr-Age 2022-07.eps

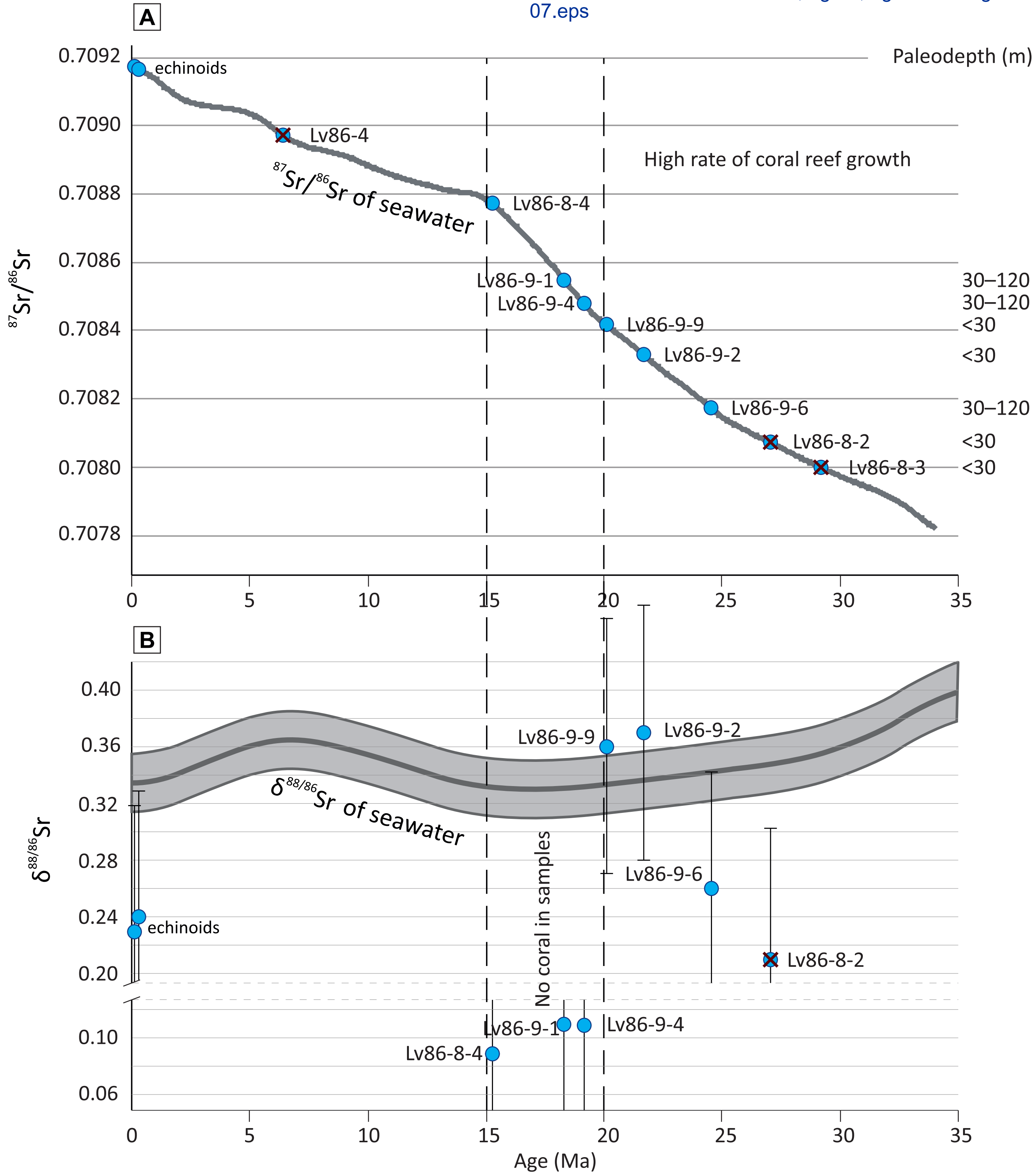

Figure 5

Click here to access/download;Figure;Fig 5 Age-Dif Age 2022-07.eps

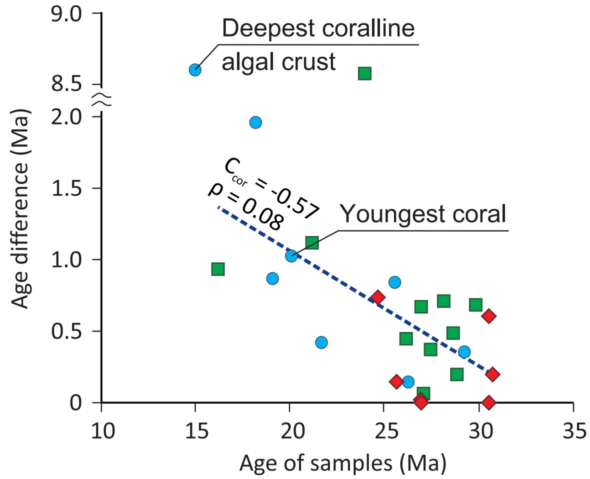

Figure 6

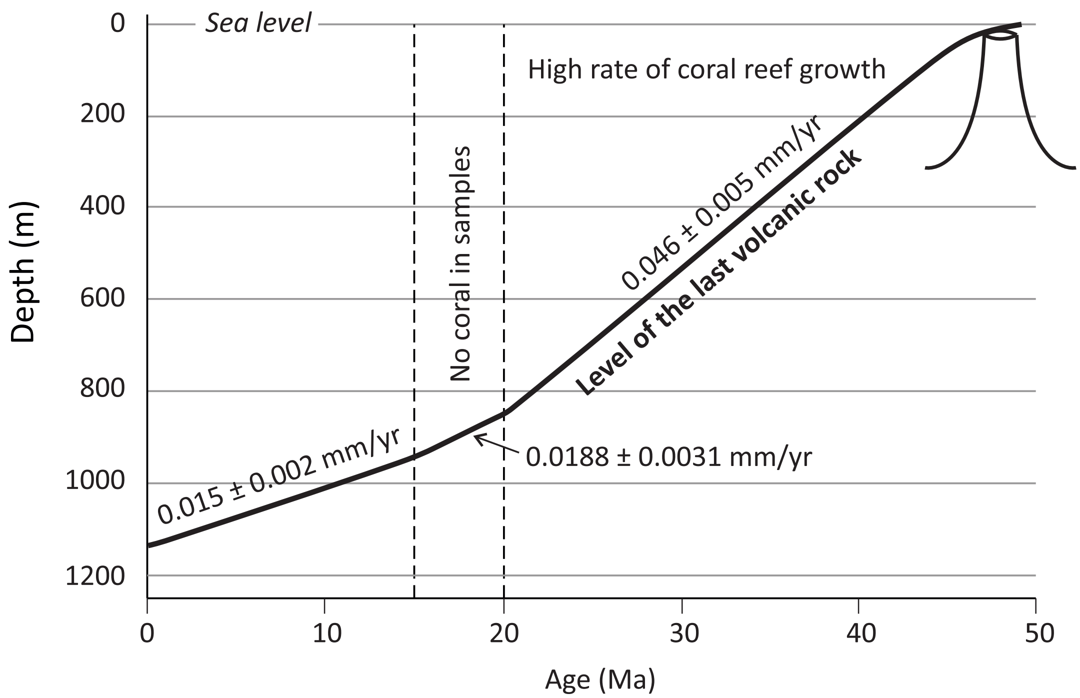

0
Sea level
200
400
600
800
1000
1200
Depth (m)
High rate of coral reef growth
No coral in samples
0.046 ± 0.005 mm/yr
Level of the last volcanic rock
0.015 ± 0.002 mm/yr
0.0188 ± 0.0031 mm/yr
0
10
20
30
40
50
Age (Ma)

Vishnevskaya et al. «Sr isotope variations…»

Table 1. Coordinates and depth of samples analysed in this study, and seawater temperature and salinity at the sampling sites.

Dive	Sample	Coordinate	Depth (m)	T (°C)	S
4	LV86-4	35.58365°N; 171.24615°E	487	10.3	34.18
4	Coral	35.71235°N; 171.07082°E	578		
8	LV86-8-2	35.71235°N; 171.07082°E	578		
8	LV86-8-3	35.71235°N; 171.07082°E	578	6.49	34
8	LV86-8-4	35.76769°N; 171.06696°E	1458	3.03	34.39
9	LV86-9 echinoid	35.65593°N; 171.05479°E	357		
9	LV86-9-1	35.65593°N; 171.05479°E	357		
9	LV86-9-2	35.65593°N; 171.05479°E	357	13.66	34.49
9	LV86-9-4	35.65625°N; 171.05437°E	374		
9	LV86-9-6	35.65699°N; 171.05472°E	360		
9	LV86-9-9	35.67756°N; 171.05456°E	357		
16	LV86-16 echinoid	35.40487°N; 171.32104°E	387	12.97	34.41

T, water temperature; S, salinity; Coral, sample of modern Isididae coral; echinoid, sample of echinoid spines

Vishnevskaya et al. «Sr isotope variations…»

Table 2. Lithology and biotic components from the studied Koko Guyot carbonate samples.

Dive	Sample	Description
8	LV86-8-2	Piece of coral Merulinidae? species
8	LV86-8-3	Rhodolith composed of encrusting coralline algae (e.g., *Lithoporella* sp.) with nuclei consisting of molluscan shells
8	LV86-8-4	Bioclastic packstone with very fine to fine sand-sized bioclasts (dominated by ostracods). Bivalves and bryozoans are subordinate
9	LV86-9-1	Larger benthic foraminifera (LBF) floatstone with coralline algal crusts (melobesioids)
9	LV86-9-2	Larger foraminiferal packstone with subordinate bryozoans, coralline algae, and bivalves. Astrea cf. annuligera are present. The matrix is composed of very fine to fine sand-sized bioclasts (rich in ostracods) with a matrix of clotted micrite
9	LV86-9-4	Fine bioclastic packstone with LBFs, coralline algal (melobesioids) fragments, and bryozoans
9	LV86-9-6	Bioclastic floatstone with gravel-sized bioclasts of LBFs (*Spiroclypeus tidoenganensis* and *Heterostegina assilinoides*), bivalves, coralline algae, and bryozoans
9	LV86-9-9	Bioclastic LBF floatstone (*Spiroclypeus tidoenganensis* and *Heterostegina* cf. *assilinoides*) and bivalves (mostly oyster), undetermined merulinid corals, and *Porites* sp.

Vishnevskaya et al. «Sr isotope variations…»

Table 3. Trace-element contents and calculated Fe/Sr and Mn/Sr ratios of the studied carbonates. Analyses were performed using ICP–AES. Contents are given in ppm.

Sample	**Fe**	**Al**	**Mn**	**Mg**	**Sr**	**Fe/Sr**	**Mn/Sr**
Coral	60	40	20	14330	2300	0.026	0.009
LV86-9 echinoid	40	110	10	4500	1300	0.031	0.008
LV86-16 echinoid	180	300	40	5470	1200	0.150	0.033
LV86-4	740	150	130	4850	1000	0.740	0.130
LV86-8-2	230	210	110	3940	300	0.767	0.367
LV86-8-3	30	80	180	3790	300	0.100	0.600
LV86-8-4	20	70	30	4230	500	0.040	0.060
LV86-9-1	10	50	10	7090	400	0.025	0.025
LV86-9-2	20	40	20	3880	230	0.087	0.087
LV86-9-4	20	60	20	4660	280	0.071	0.071
LV86-9-6	10	60	30	3410	300	0.033	0.100
LV86-9-9	10	50	30	3860	300	0.033	0.100

Vishnevskaya et al. «Sr isotope variations…»

Table 4. Strontium isotope compositions and ages according to LOWESS 3 (McArthur et al., 2001, 2012).

Sample	$\delta^{88/86}$Sr (‰)	SE, abs	^{87}Sr/^{86}Sr	SE, abs	Minimum age (Ma)	Maximum age (Ma)	Median age (Ma)
Coral	−0.06	0.01	0.709108	0.000008			
LV86-9 echinoid	0.24	0.01	0.709174	0.000007			
LV86-16 echinoid	0.23	0.01	0.709173	0.000008			
LV86-4	−0.05	0.01	0.708961	0.000006	6.40	7	6.70
LV86-8-2	0.21	0.01	0.708064	0.000007	26.85	27.75	26.30
LV86-8-3	−0.03	0.01	0.708000	0.000006	28.75	29.65	29.20
LV86-8-4	0.09	0.01	0.708771	0.000006	15.10	15.45	15.30
LV86-9-1	0.11	0.01	0.708557	0.000006	18.05	18.35	18.20
LV86-9-2	0.37	0.01	0.708330	0.000010	21.35	21.95	21.65
LV86-9-4	0.11	0.01	0.708482	0.000006	19.05	19.10	19.07
LV86-9-6	0.26	0.04	0.708173	0.000020	24.05	25.10	25.55
LV86-9-9	0.36	0.01	0.708415	0.000006	19.85	20.40	20.10

SE, standard error in absolute value

Vishnevskaya et al. «Sr isotope variations…»

Table 5. Strontium isotope ages of samples from the present study and previous studies (blue, Grigg, 1988; yellow, Tarduno et al., 2003; green, Clague et al., 2010; white, this study) used to calculate age differences between consecutive samples.

						Ranked data			
Sample	Age (Ma)	error	Paleodepth (m)	Modern depth (m)		Sample	Age (Ma)	error	Age difference (Ma)
this work						LV86-4	6.7	0.30	
LV86-4	6.7	0.3	>120	487		LV86-8-4	15.30	0.15	8.60
LV86-8-4	15.30	0.15	30–120	1458		A8	16.24	0.15	0.94
LV86-9-1	18.20	0.15	30–120	357		LV86-9-1	18.20	0.21	1.96
LV86-9-4	19.07	0.03	30–120	374		LV86-9-4	19.07	0.03	0.87
LV86-9-9	20.1	0.30	30	357		LV86-9-9	20.1	0.30	1.03
LV86-9-2	21.65	0.30	30–120	357		A23	21.22	0.22	1.12
LV86-9-6	25.55	0.45	30–120	360		LV86-9-2	21.65	0.30	0.43
LV86-8-3	29.2	0.50	30–120	578		A26	23.96	0.28	2.31
LV86-8-2	26.3	0.50	30	578		Favia sp. 1	24.7		0.74
Grigg, 1988						LV86-9-6	25.55	0.45	0.85
Favia sp. 1	24.7		20	624–823		Favia sp. 2	25.7		0.15
Favia sp. 2	25.7		20	624–823		A32	26.15	0.50	0.45
	30.7		20	624–823		LV86-8-2	26.3	0.50	0.15
Favites sp. 1	27		20	624–823		A22	26.97	0.43	0.67
Favites sp. 2	30.5		20	624–823		Favites sp. 1	27		0.03
Platygyra sp.	30.5		20	624–823		Seriatopora sp.	27		0.00
Seriatopora sp.	27		20	624–823		A12	27.07	0.47	0.07
Clague et al., 2010						A18	27.44	0.44	0.37
A5	28.64		20	624–823		A19	28.15	0.33	0.71
A6	29.89	0.43	20	624–823		A5	28.64		0.49
A8	16.24	0.21	120	624–823		A20	28.84	0.36	0.20
A12	27.07	0.47	20	624–823		LV86-8-3	29.2	0.50	0.36
A18	27.44	0.44	20	624–823		A6	29.89	0.43	0.69
A19	28.15	0.33	20	624–823		Favites sp. 2	30.5		0.61
A20	28.84	0.36	20	624–823		Platygyra sp.	30.5		0.00
A22	26.97	0.43	20	624–823			30.7		0.20
A23	21.22	0.22	20	624–823		Oldest sediment	43.5		12.80
A26	23.96	0.28	20	624–823					
A32	26.15	0.50	20	624–823					
Tarduno et al., 2003									
Oldest sediment	43.5								

Declaration of interests

☐The authors declare that they have no known competing financial interests or personal relationships that could have appeared to influence the work reported in this paper.

☒The authors declare the following financial interests/personal relationships which may be considered as potential competing interests:

Vishnevskaya Irina A., Mikhailik Pavel E. reports equipment, supplies and travel were provided by A.V. Zhirmunsky National Scientific Centre of Marine Biology FEB RAS (Vladivostok).

Sr isotope variations in Oligocene–Miocene and modern biogenic carbonate formations of Koko Guyot (Emperor Seamount Chain, Pacific Ocean)

Irina A. Vishnevskaya [a,b,*], Marc Humblet [c], Yasufumi Iryu [d], Davide Bassi [e], Tatiana G. Okuneva [f], Daria V. Kiseleva [f], Andrey V. Vishnevskiy [b, g], Natalia G. Soloshenko [f], Pavel E. Mikhailik [h]

[a] Vernadsky Institute of Geochemistry and Analytical Chemistry, RAS, 119334 Moscow, 19 Kosygina str., Russia

[b] Novosibirsk State University, 630090 Novosibirsk, 1 Pirogova str., Russia

[c] Nagoya University, Department of Earth and Planetary Sciences, 464-8601 Nagoya, Japan

[d] Institute of Geology and Paleontology, Graduate School of Science, Tohoku University, Aramaki-aza-aoba 6-3, Aoba-ku, Sendai 980-8578, Japan

[e] Dipartimento di Fisica e Scienze della Terra, Università degli Studi di Ferrara, Via Saragat 1, I-44122, Ferrara, Italy

[f] Zavaritsky Institute of Geology and Geochemistry, UB RAS, 620016 Ekaterinburg, 15 Akademika Vonsovskogo str., Russia

[g] Sobolev Institute of Geology and Mineralogy, SB RAS, 630090 Novosibirsk, 3 Akademika Koptyuga ave., Russia

[h] Far East Geological Institute, Far East Branch of Russian Academy of Sciences (FEGI FEB RAS), Prospekt 100-letiya, 159, 690022 Vladivostok, Russia

* Corresponding author:

E-mail address: vishnevskaia@geokhi.ru, vishnevskaia.i.a@gmail.com (I.A. Vishnevskaya).

ABSTRACT

The Hawaiian–~~-~~Emperor Seamount Chain, a major topographic feature of the Pacific Ocean floor, is composed of seamounts capped with fossil coral reef deposits that ~~formed~~ originally formed close to sea level but are now ~~lying today~~covered by hundreds of meters ~~in~~ of water ~~depth due~~owing to prolonged subsidence. These fossil reef deposits are important archives of paleoenvironmental change~~s~~ and yield information on the subsidence history of the seamounts. We studied the Sr isotope compositions of Oligocene–Miocene coral reef limestone from Koko

Formatted: English (United States)

Formatted: English (United States)

Formatted: English (United States)

Guyot in the southern ~~part of the~~ Emperor Seamount Chain ~~in order~~ to assess the dynamics of the subsidence ~~dynamics~~. ~~The age~~The ages of the studied samples ~~with~~ containing coral fragments established by Sr isotope stratigraphy vary~~ies~~ from 26.3 to 20.1 Ma. In contrast, ~~, while~~ the youngest samples (15.3 Ma), which were deposited ~~at~~ in water depths of ~~water depth of~~ >-120 m, are barren ~~in~~ of corals and are composed exclusively of bryozoans and coralline algae~~, are 15.3 Ma in age~~. The subsidence rate of the Koko Guyot volcanic structure was not ~~uniform~~constant over time. ~~Combining data of previous studies and those obtained in this study,~~Integration of our new data with the results of previous studies reveals that the ~~assessed~~ subsidence rate was 0.046 ±– 0.005 mm/yr during the first 25–30 Myr (from 49–44 to 20 Ma~~c.from 49–44 Ma~~). During this period ~~of time~~, Koko Guyot was in a bathymetric interval favo~~u~~rable for coral reef development, -and its subsidence was compensated by rapid vertical growth of the reef ~~growth~~. ~~Successively~~Subsequently, the subsidence rate decreased to an average value of 0.019 ± 0.003 mm/yr from 20 to 15 Ma. The decrease in the rate of bottom subsidence coincided with unfavo~~u~~rable environmental conditions for coral reef development, leading to the disappearance of corals. The average subsidence rate ~~reached a value of~~has been 0.015 ± 0.002 mm/yr ~~in the last~~since 15 Ma, comparable ~~to~~ to the present-day subsidence rate. ~~The $\delta^{88/86}$Sr value of the studied samples, which are represented by fragments of warm-water corals and formed 25–20 Ma ago, corresponds to that in the generalized $\delta^{88/86}$Sr variation curve in the World Ocean (0.32±0.1‰ *vs.* 0.34±0.03‰). More recent carbonates, which are formed by Larger benthic foraminifera, and coralline algal, and other non-coral species, have $\delta^{88/86}$Sr well below this curve (about 0.10±0.09‰ *vs.* 0.33±0.02‰), which we attribute this fractionation to change in environmental and in biocommunity.~~ We also analyzed the stable Sr isotope ratios ($\delta^{88/86}$Sr) of warm-water coral samples formed at 25–20 Ma (0.32‰ ± 0.1‰), as well as carbonate of large benthic foraminifera, coralline algae, and other non-coral species for the period 20–15 Ma (0.10‰ ± 0.09‰). We suggest that the large difference in carbonate $\delta^{88/86}$Sr between 25–20 and 20–15 Ma corresponds to a difference in the fractionation factor caused by environmental and benthic community change.

Key words:
^{87}Sr/^{86}Sr ratio, $\delta^{88/86}$Sr, Corals, Bryozoans, Larger foraminifera, Subsidence, Hawaiian–Emperor Seamount Chain, Hawaiian hotspot

1. Introduction

Formatted: English (United States)
Formatted: English (United States)
Formatted: English (United States)
Formatted: English (United States)
Formatted: English (United States)
Formatted: English (United States)
Formatted: Underline, English (United States)
Formatted: Underline, English (United States)
Formatted: English (United States)
Formatted: English (United States)
Formatted: English (United States)
Formatted: English (United States)
Formatted: English (United States)
Formatted: English (United States)
Formatted: English (United States)
Formatted: English (United States)
Formatted: English (United States)
Formatted: English (United States)
Formatted: English (United States)
Formatted: English (United States)
Formatted: English (United States)
Formatted: English (United States)
Formatted: English (United States)
Formatted: English (United States)
Formatted: English (United States)
Formatted: English (United States)
Formatted: English (United States)
Formatted: English (United States)
Formatted: English (United States)
Formatted: English (United States)
Formatted: Russian
Formatted: English (United States)

The Emperor Seamount Chain (Pacific Ocean) includes more than a dozen seamounts (i.e., extinct volcanoes). The northernmost seamount of ~~-~~Meiji ~~-Seamount~~ is considered the oldest, with an age estimated at 85 Ma (Keller et al., 2000). The youngest seamount of Daikakuji ~~Seamount~~ (42 Ma; Dalrymple and Clague, 1976) is located at the junction of the Emperor Seamount Chain with the Hawaiian Seamount Chain (Fig. 1). Koko Guyot is the southernmost seamount and one of the largest in the Emperor Seamount Chain with a surface area of 5.800 km^2 (Greene et al., 1980). It is located from 34º to 36.5º N and from 170.8º to 171.5º E. The top of the guyot, located at a depth of 270 m from the sea level (Matter, Gardner, 1975), is characterize by a predominantly flat upper part at 300–400 m water depth.

The Emperor–Hawaiian Seamount Chain formed as a result of the prolonged activity of the so-called Hawaiian ~~Hot Spot~~hotspot, a long-lived mantle plume beneath the Pacific Plate (Jackson et al., 1980; Clague and Dalrymple, 1987; Tarduno et al., 2003; and references therein). Plate movement relative to conventionally stationary mantle structure led to the formation of a linear chain of volcanic islands and seamounts with ages increasing from south to north. The seamounts situated in ~~the south of the~~the southern Emperor Seamount Chain are topped with a sediment cover containing carbonate rocks (Shipboard Scientific Party, 1975a, 1975b, 2002), which represent an excellent geochemical, paleontological, and paleogeographic settings.

The following development sequence for seamounts has been established (Wheeler and Aharon, 1991). After the cessation of volcanic activity, a coral reef began to develop on the volcanic island ~~(Wheeler and Aharon, 1991)~~. Over time, the volcano subsided, and the coral reef at first kept pace with relative sea-level rise by enlarging upward. As the oceanic crust moved away from the area of plume activity and cooled, the volcano subsided further, and the coral reef (which was unable to keep up with sea-level rise) drowned. ~~The~~ Although the main cause of ~~drowning~~ the demise of the coral ~~could be~~was the rapid ~~a~~ relative sea-level rise ~~to, o fast for the coral reef to keep up, but it could also be related to the~~other factors such as a decrease in sea surface temperature, as the volcanic island migrated to higher latitudes by plate motion may also have been influential (e.g., Clague et al., 2010) ~~decrease in sea surface temperature (SST) as the volcanic island migrated to higher latitudes or combination of several factors (e.g., Clague et al. (2010)): migration in cooler waters, global cooling trend, combined with slow subsidence.~~

~~Based on all available information, the speed and direction of movement of the hotspot and the Pacific plate have been established. Koko Guyot and the hotspot diverged in different directions: the seamount to the north, the hotspot to the south (Wilson, 1963; Clague and Dalrymple, 1987; Tarduno et al., 2003). Clague et al. (2010) studied corals in southern Koko Guyot, and used Sr isotope stratigraphy to date the carbonates. According to their calculation, in the first 5 Ma of its existence, Koko Guyot was migrating at a rate of 69 km Myr~~$^{-1}$ ~~and the guyot~~

~~moved from 21.5°N to 23°N. In addition, the authors also show that the rate at which Koko Guyot migrated decreased to 31 km Myr^{-1} between 45 Ma and the present, and that the direction of movement changed to the north-west before reaching its present position at latitude 35°N. Clague et al. (2010) propose a two-phase subsidence history: (1) ~0.009 mm yr^{-1} from 27.1 to 16.2 Ma, and (2) ~0.014 mm yr^{-1} from 16.2 Ma to the present. They also suggest that the timing of reef growth cessation at Koko Guyot occurred around 29 Ma, based on the youngest age of corals they sampled (i.e., 27 Ma), and the average subsidence rate they calculated (i.e., 0.012 mm yr^{-1}).~~ Data regarding the speed and direction of movement of the Hawaiian hotspot and the Pacific Plate show that the paths of Koko Guyot and the hotspot diverged (*c.* 45 Ma), whereby the seamount moved to the north and the hotspot moved to the south (Wilson, 1963; Clague and Dalrymple, 1987; Tarduno et al., 2003). Clague et al. (2010) studied corals in southern Koko Guyot and used Sr isotope stratigraphy to date the carbonates. According to those authors' calculations, Koko Guyot migrated northward at a rate of 69 km/Myr during the first 5 Myr (*c.* 50–45 Ma) of its existence, moving from 21.5° to 23°N. In addition, the rate at which the guyot migrated decreased to 31 km/Myr between 45 Ma and the present, and the direction of movement changed to the northwest before reaching its present position at 35°N. Clague et al. (2010) proposed a two-phase subsidence history for Koko Guyot: (1) ~0.009 mm/yr from 27.1 to 16.2 Ma; and (2) ~0.014 mm/yr from 16.2 Ma to the present. Those authors also suggested that the timing of reef growth cessation at Koko Guyot occurred at *c.* 29 Ma, on the basis of the youngest age of sampled corals (27 Ma) and the calculated average subsidence rate (0.012 mm/yr).

~~We studied samples from the northwestern part of the Koko Guyot, where sampling had not been carried out so far. We used a new sampling method for this region – a remotely controlled underwater vehicle (see Methods), so our samples are geographically and bathymetrically referenced. As part of our study, we did not want to refute previous studies, we wanted to check them and, if possible, improve them, which is why the samples were taken from a place remote (but not very much) from the area of previous works. The aim of this study is to establish the youngest age limit of coral reefs on Koko Guyot, and to perform further constrains of the timing of coral reef drowning as Koko Guyot was submerged. Moreover, in order to improve the understanding of the subsidence history of Koko Guyot, we use the difference in the age of sampled corals and their bathymetry to calculate the average subsidence rate of this volcanic structure. To achieve these goals, we performed a paleontological analysis and a study of the Sr isotope composition of samples collected from the Koko Guyot. We compared the obtained $^{87}Sr/^{86}Sr$ ratios with the curve of variation of this value in the Cenozoic (McArthur et al., 2001, 2020). In addition, we use the $\delta^{88/86}Sr$ record measured in carbonates as a proxy for an~~

~~environmental change on the flooded reef platform.~~ We studied samples obtained from the northwestern part of Koko Guyot, where sampling has hitherto not been conducted. We used a new sampling method for this region, namely, a remotely controlled underwater vehicle (see "Material and Methods"), so our samples could be geographically and bathymetrically referenced. Our purpose was to confirm the previous estimates of coral age and subsidence rate made by Clague et al. (2010) with samples taken from a site distant from the area of previous work and, if possible, improve the estimates by measuring isotope ratios using a different type of equipment (a Neptune Plus multicollector inductively coupled plasma mass spectrometry (ICP–MS) instrument versus a VG Sector 54 Thermal ionization mass spectrometer (TIMS) in Clague et al. (2010)) and reducing uncertainties in age estimates. The aim of the study was to establish the youngest age limit of coral reefs on Koko Guyot and further constrain the timing of coral reef drowning as Koko Guyot became submerged. In addition, to improve the understanding of the subsidence history of Koko Guyot, we used differences in the ages of sampled corals and their depths to calculate the average subsidence rate of this volcanic structure for different periods. To achieve these aims, we performed paleontological analysis and measured the Sr isotope compositions of samples collected from the Koko Guyot. We compared the obtained $^{87}Sr/^{86}Sr$ ratios with the variation curve of this ratio for the Cenozoic (McArthur et al., 2001, 2020). In addition, we used the $\delta^{88/86}Sr$ record measured in carbonates as a proxy for environmental change on the flooded reef platform.

Formatted: English (United States)

Formatted: English (United States)

2. Materials and methods

The 86th voyage of the research vessel "Akademik M.A. Lavrentiev" ~~research vessel~~ was held ~~in~~ during July–August 2019. The aim of the expedition was to conduct a comprehensive study of the seamounts of the southern ~~part of the~~ Emperor Seamount Chain. ~~Koko Guyot is the southernmost seamount and one of the largest in the Emperor Seamount Chain with a surface area of 5.800 km² (Greene et al., 1980). It is located from 34° to 36.5° N and from 170.8° to 171.5° E. The top of the guyot, located at a depth of 270 m from the sea level (Matter, Gardner, 1975), is characterize by a predominantly flat upper part at 300–400 m water depth.~~ The subject of ~~this research~~the present study, the southernmost and ~~the~~ youngest seamount of the Emperor Seamount Chain (i.e., Koko Guyot), is an isolated underwater volcanic seamount with a flat top lying more than 300 m below ~~the~~ present mean sea level. ~~It~~The guyot- is composed mainly of alkaline basalts with minor ~~and, to a lesser extent,~~ tholeiitic basalts (Clague and Dalrymple, 1987). The final stage of eruptions is represented by ~~an interlayering of~~interlayered pahoehoe

Formatted: English (United States)

Formatted: English (United States)

Formatted: English (United States)

flows, subaerial aa units, and flow foot breccias. ~~In~~ During the course of previous ~~studies,~~studies as part of the Deep Sea Drilling Program (DSDP) and Ocean Drilling Program (ODP), several sediment cores were recovered: DSDP Leg 32 sites 308 and 309 (Shipboard Scientific Party, 1975a, 1975b) and ODP Leg 197 Site 1206 (Shipboard Scientific Party, 2002). ~~The studied collected material allowed the earliest sedimentation stages and, accordingly, the waning of volcanic activity to be investigated. The fossil benthic assemblages, the paleoenvironmental setting and the age were also assessed. At the ODP Site 1206, the lava flows are separated by limestone and volcanoclastic sandstone layers (Tarduno et al., 2003), which indicate the near-surface nature of the eruptions.~~ The materials collected during those expeditions allowed the earliest sedimentation stages and waning of volcanic activity to be investigated, as well as fossil benthic assemblages, paleoenvironmental setting, and ages volcanic and sedimentary rocks. At ODP Site 1206, lava flows are separated by limestone and volcaniclastic sandstone layers (Tarduno et al., 2003), suggesting the near-surface nature of the eruptions. The age of the volcanic edifice of the Koko Guyot is estimated ~~to be~~as ~~about~~ 49–48 Ma (Jackson et al., 1980; Tarduno et al., 2003; Duncan and Keller, 2004). The minimum age of the Koko eruptions ~~is~~ has been determined from nannofossils occurring at the base of the sedimentary cover, which probably overlaps the last lava flow, and coincides with biozones NP14 and NP15 (~~(~~middle Eocene; Speijer et al., 2020). A seismic survey of the Koko Guyot has shown that the volcanic structure is covered by a ~~ca.~~ ~600~~-~~m-thick carbonate cap associated with coral reef deposits (Davies et al., 1972). The exposed sedimentary part of ~~the section of a~~ drill cores from DSDP sites 308 and 309 is composed of altered volcanoclastic siltstones and sandstones with a sharp contact between them. The sandstones contain bioclasts ~~represented of~~by bryozoans, solitary corals, ostracods, coralline algae, benthic foraminifera, ~~molluscs~~mollusks, and ooids. The fossil assemblage indicates an early ~~lower~~ Eocene shallow-water setting (Larson et al., 1975).

The materials collected for the present study were ~~The rock material was~~ collected using a remotely operated underwater vehicle (~~of the~~ Comanche ~~type,~~ ~~(~~SUB-Atlantic, UK), equipped with Schilling Robotics Orion hydraulic manipulators, and a Sonardyne hydroacoustic positioning system coupled with a GPS navigation system. During ~~the cruise,~~ the voyage, 11 dives were performed to survey the top and slopes of Koko Guyot. Carbonate material was collected during four dives, three of which ~~were located~~were performed on the northwestern peak of the guyot (dives 4, 8, and 9; Fig. 1) and the fourth in the western part of the main plateau (dive 16; Fig. 1). ~~In addition, a~~A living deep-sea ~~Isidid~~ isidid octocoral, also ~~called~~ termed "bamboo coral", was collected during dive 4. We used this octocoral~~it~~ as a reference ~~of~~ for modern carbonate accumulation. Sampling points and physical water characteristics are ~~shown~~ presented in Fig. 1 and Table 1. Carbonate rocks were collected directly with a manipulator

Formatted: English (United States)
Formatted: English (United States)
Formatted: English (United States)
Formatted: English (United States)
Formatted: English (United States)
Formatted: English (United States)
Formatted: English (United States)
Formatted: English (United States)
Formatted: English (United States)
Formatted: English (United States)
Formatted: English (United States)
Formatted: No underline, English (United States)
Formatted: English (United States)
Formatted: English (United States)
Formatted: English (United States)
Formatted: English (United States)

operated from the surface (Fig. 2A~~a~~) and with a 15~~×~~ cm × 15 cm scoop net (Fig. 2B~~b~~). ~~In the first case~~For rocks collected by the manipulator, a ~~the rock samples were large enough and a block~~block measuring 1.5~~×~~ cm × 1.5 cm~~×~~ × 1.5 cm in size ~~was~~ was cut from the~~ir~~ central part of each rock sample. These cubes were passed through a magnet to remove any metal shavings from the saw and ~~were~~ washed in distilled water. ~~During the latter operation~~For material collected by the scoop net, the ~~the~~ sediment was washed with seawater and sorted into different grain-size fractions from 1 ~~mm~~ to 50 mm. After careful visual inspection, the ~~most~~ lightest-colo~~u~~red and unaltered samples devoid of Fe–Mn oxide–hydroxide coatings were selected for geochemical analyses. The selected samples were washed with a brush in running water and finally rinsed in distilled water. All samples were photographed directly on board.

Further sample preparation was carried out in the cleanrooms (class 1~~,~~000) and laminar boxes (class 100) of the Laboratory o~~O~~f Physical a~~A~~nd Chemical Methods o~~O~~f Analysis, the Zavaritsky Institute of Geology and Geochemistry UB RAS, Ekaterinburg, Russia.

Fragments of carbonate rocks without an outer crust and individual parts of fossils weighing about 100 mg were washed three times in ultrapure water (AriumPro, Sartorius). Then, 5 ml of 1N HCl were added. ~~Complete~~Although complete dissolution of all the material ~~was observed~~occurred ~~in~~ during the first few minutes, ~~but~~ the samples were left in the acid for 24 ~~hours~~ h at room temperature. ~~Then the~~The solution was then centrifuged for 20 ~~minutes~~ min at 6~~,~~000 rpm ~~by~~ in an EBA 21 centrifuge (Hettich, Germany). The resulting ~~, and the~~ supernatant was taken ~~exactly~~ from the central part of the liquid column so that ~~the~~ undissolved residue containing the flakes of ~~possibly~~ possible organic matter would not enter the resulting liquid. ~~The following measurements~~Measurements ~~demonstrated~~ showed that Fe and Mn contents were ~~was~~ less than 50 ppm and less than 20 ppm in the majority of the samples, respectively. These values are~~is is~~ consistent with ~~the~~ data for the lattice phases of foraminiferal calcite from Palmer (1985) and provide evidence~~d~~ for the lack of secondary Fe–Mn oxide–hydroxides in the studied solutions. The resulting liquid was divided into two aliquots: 2 ml ~~were~~ was transferred to test tubes for elemental analysis, and the rest of the liquid was ~~left~~ retained for Sr ~~isotopic~~ isotope analysis.

An ~~inductively coupled plasma~~ICP–atomic emission spectrometry (AES) instrument (Optima-8000 DV, PerkinElmer, USA~~; ICP-AES~~) was used to determine major-element~~al~~ compositions, ~~such as~~including Mg, Mn, Sr, and Al, as well as ~~the~~ traces of Fe. C~~The c~~ontrol of the accuracy and precision of ~~determining the~~ major- and trace-element compositions was ~~carried out~~performed using IAG/CGL 020 ML-3 certified limestone provided by the Central Geological Laboratory of Mongolia. The ~~concentrations~~ contents of major and trace elements were measured on a regular basis during 2019, yielding the following ~~concentration~~contents: Fe

Formatted: English (United States)
Formatted: English (United States)
Formatted: English (United States)
Formatted: English (United States)
Formatted: English (United States)
Formatted: English (United States)
Formatted: English (United States)
Formatted: English (United States)
Formatted: English (United States)
Formatted: English (United States)
Formatted: English (United States)
Formatted: English (United States)
Formatted: English (United States)
Formatted: English (United States)
Formatted: English (United States)
Formatted: English (United States)
Formatted: English (United States)
Formatted: English (United States)

= 2350 ± 350 ppm, Al = 6000 ± 900 ppm, Mn = 180 ± 30 ppm, Mg = 8400 ± 1260 ppm, and Sr = 1000 ± 150 ppm (2SD, N = 30). The o~~O~~btained ~~concentration~~contents were in good agreement with the certified values ~~for~~ of Fe = 2400 ± 100 ppm, Al = 6100 ± 100 ppm, Mn = 178 ± 8 ppm, Mg = 8350 ± 145 ppm, and Sr = 1018 ± 30 ppm (Certificate of analysis IAG / CGL 020 ML-3 (Limestone), 2015)~~(Certificate of analysis…, 2015)~~. The precision of each individual result (relative standard deviation or RSD) ~~during the sample measurement~~ was ~~within~~ better than 1%.

The volumes of liquid samples calculated to match ~~c.~~ ~300 ppb of Sr were placed in a PFA vial and evaporated to dryness on a hotplate at 120 °C. ~~Then, the~~The residue was dissolved in 0.5 mL of 7 M HNO_3, placed in an Eppendorf microtube, and centrifuged at 6~~,~~000 rpm for 15 min by an EBA 21 centrifuge (Hettich, Germany). A s~~S~~ingle-step chromatography technique using SR-Resin (100–200 mesh, Triskem®, TrisKem International, France) was applied for ~~strontium~~ Sr isolation (Vishnevskaya et al., 2020). Purified Sr fraction was evaporated to dryness and dissolved with 3% HNO_3 (v/v) for further isotope ratio measurement.

Stable Sr isotopic compositions have been measured in other studies using both TIMS and MC–ICP–MS (McArthur et al., 2020; Teng et al., 2017). The d~~D~~ouble-spike (DS) technique is usually applied for TIMS (Krabbenhö~~o~~ft et al., 2009; Shalev et al., 2013; Paytan et al., 2021) and MC–ICP–MS (Shalev et al., 2013), although ~~more~~ MC–ICP–MS ~~MC-ICP-MS~~ analytical protocols have tended to adopt~~ed~~ ~~the~~ standard-sample bracketing (SSB) MC–ICP–MS ~~MC-ICP-MS~~ (Fietzke and Eisenhauer, 2006; Moynier et al., 2010; Charlier et al., 2012; Ma et al., 2013). ~~Generally~~In general, ~~the~~ DS TIMS is considered to have the highest precision and accuracy, followed by DS MC–ICP–MS ~~MC-ICP-MS~~ and SSB MC–ICP–MS ~~MC-ICP-MS~~ ~~(Teng et al., 2017)~~.

Radiogenic and stable Sr isotopes were measured in this study using an ~~multicollector-inductively coupled plasma mass spectrometer (MC–ICP–MSMC-ICP-MS)~~ Neptune Plus instrument (Thermo Fisher Scientific, Germany). The mass bias was corrected using ~~the~~ a combination of exponential law normalization ($^{87}Sr/^{86}Sr = 8.37861$) and bracketing, with ~~technique (~~the normalized values ~~were~~ being additionally corrected by the mean reference value of 0.710245 for SRM-987 strontium carbonate (GeoReM database, http://georem.mpch-mainz.gwdg.de/)~~)~~. ~~In order to control~~To monitor the analytical procedure, SRM-987 was measured on a regular basis, yielding $^{87}Sr/^{86}Sr = 0.710261 \pm 0.000020$ (2SD, N = 257). The precision of the determinations ~~method precision~~ estimated as ~~the~~ the within-laboratory standard uncertainty (2σ) obtained for SRM-987 was ±0.003 %. The precision of each individual result (1σ ~~SE~~) during the sample measurement was ~~within~~ better than ±20 ppm. Long-term analyses of $\delta^{88/86}Sr$ in SRM-987 processed through chromatographic columns and measured as unknowns

Formatted: English (United States)

Formatted: Underline, English (United States)

Formatted: English (United States)

Formatted: English (United States)

yielded ~~−~~−0.01‰ ± ~~−~~ 0.09‰ (2SD, N~~=~~ = 34). ~~Additionally~~In addition, NIST SRM 1400 bone ash was analyzed as $\delta^{88/86}$Sr = ~~−~~−0.33‰ ± ~~-~~0.09‰ (2SD, N~~=~~ = 10), ~~; this value was~~ in agreement with ~~that~~ the value provided in the GeoReM database. The precision of each individual result (1σ ~~SE~~) ~~during the sample measurement~~ was ~~within~~ better than ±0.006‰.

3. Results

The studied samples ~~are represented by~~are composed of limestone with a fine-grained matrix (micrite), containing abundant biogenic components (corals, coralline algae, molluscs, and benthic foraminifera) and undetermined carbonate fragments. Several samples contain fossil corals, including *Astrea* cf. *annuligera* Milne Edwards & Haime, 1849,~~;~~ *Porites* sp., ~~-~~and at least one other undetermined Merulinidae (Table 2 and ~~,~~Fig. 3). Large benthic foraminifera (LBF) represented by *Spiroclypeus tidoenganensis* Van der Vlerk, 1925 and *Heterostegina* cf. *assilinoides* (Blanckenhorn) Henson, 1937 occur in samples Lv86-9-6, Lv86-9-2, and Lv86-9-9 ~~samples~~ (sample numbers are given ~~in the ascending age order~~ from ~~the~~ oldest to ~~the~~ youngest). Samples LV86-9 and LV86-16 ~~samples~~ consist of cidaroid echinoderm spines (identified by Dr. K.V. Minin, Shirshov Institute of Oceanology of Russian Academy of Sciences; Fig. 3B). The studied samples have a good degree of preservation, ~~degree of the studied samples based on~~as assessed by optical examination ~~is good~~.

In general, u~~U~~nder the influence of post-sedimentary fluids, Fe and Mn contents increase and Sr and Mg decrease in carbonates (Veiser, 1983; Banner, 2004; Sawaki et al., 2010). Consequently, by studying the mutual correlations of these elements, it is possible to ~~select~~ identify samples that have been ~~the~~ least affected by diagenetic alteration~~s~~. ~~In the case when~~Samples with low ~~the chemical composition has not changed, the~~ Mn/Sr and~~,~~ Fe/Sr ratios are ~~are low~~interpreted as not having undergone~~.~~ ~~We believe that such samples did not undergo~~ diagenetic processes, meaning that their ~~and their~~ isotope characteristics ~~are close to~~faithfully record those of the primary ~~sedimentary ones~~materials. The contents of Fe, Mn, Al, Sr, and Mg ~~concentrations~~ in our samples~~,~~ are very low, except in three samples (Table~~.~~ 3). The Fe/Sr ratio is particularly high in samples LV86-4 and LV86-8-2 ~~samples~~, with values of 0.74 and 0.77, respectively (Table 3). Sample LV86-8-2 ~~sample has also~~also has a high Mn/Sr ratio (0.37), as does ~~. A high Mn/Sr ratio (0.60) is characteristic of~~ LV86-8-3 (0.60). ~~sample as well.~~ These three samples (LV86-4, LV86-8-2, and LV86-8-3), for which at least one of the two ratios (Mn/Sr and~~,~~ Fe/Sr) is high, are used with caution in our interpretations~~analysis~~, and the isotopic data derived from them are considered less reliable compared with other samples.

Formatted: English (United States)
Formatted: English (United States)
Formatted: English (United States)
Formatted: English (United States)
Formatted: English (United States)
Formatted: English (United States)
Formatted: English (United States)
Formatted: English (United States)
Formatted: English (United States)
Formatted: English (United States)
Formatted: English (United States)
Formatted: English (United States)
Formatted: English (United States)
Formatted: English (United States)

~~The Sr isotope composition of two calcified echinoderm spines are very close (0.70917, $\delta^{88/86}$Sr 0.24 ‰). LV86-4, LV86-8-2, and LV86-8-3 samples, apparently transformed in the course of secondary processes, have ^{87}Sr/^{86}Sr ratios of 0.708961, 0.708064, and 0.708000, respectively. The Sr isotope composition of the remaining limestones range from 0.70817 to 0.70877, with a mean value of 0.70845 (Table 4). Their δ88/86Sr varies from 0.09 up to 0.37 ‰ with a mean value of 0.22 ‰. An inverse relationship is observed between $\delta^{88/86}$Sr and ^{87}Sr/^{86}Sr (correlation coefficient*, Ccor = - 0.69), and a direct relationship between the isotopic composition and Sr content (Ccor = 0.75).~~

~~* here and below the equation for calculating the correlation coefficient is:~~

$$Correl(X,Y)=\frac{\sum(x-\bar{x})(y-\bar{y})}{\sqrt{\sum(x-\bar{x})^2\sum(y-\bar{y})^2}}$$

~~when $\bar{x}$ and $\bar{y}$ are mean values of two arrays.~~

The Sr isotope compositions of two calcified echinoderm spines are very similar (^{87}Sr/^{86}Sr = 0.70917 ± 0.000008, $\delta^{88/86}$Sr 0.24 ± 0.01‰). Samples LV86-4, LV86-8-2, and LV86-8-3, which we infer to have undergone a degree of diagenetic alteration, have ^{87}Sr/^{86}Sr ratios of 0.708961, 0.708064, and 0.708000, respectively. The ^{87}Sr/^{86}Sr ratios of the remaining limestones range from 0.70817 to 0.70877, with a mean value of 0.70845 (Table 4), and their $\delta^{88/86}$Sr values vary from 0.09‰ to 0.37‰, with a mean value of 0.22‰. An inverse relationship is observed between $\delta^{88/86}$Sr and ^{87}Sr/^{86}Sr (correlation coefficient, $C_{cor} = -0.69$, $\rho = 0.13$), meaning that $\delta^{88/86}$Sr decreases with decreasing Sr isotopic age. There is a positive relationship between isotopic composition and Sr content ($C_{cor} = 0.75$, $\rho = 0.08$). Here and below, the correlation coefficient is calculated as

$$Correl(X,Y)=\frac{\sum(x-\bar{x})(y-\bar{y})}{\sqrt{\sum(x-\bar{x})^2\sum(y-\bar{y})^2}}$$

where $\bar{x}$ and $\bar{y}$ are mean values of two arrays.

4. Discussion

4.1. ~~Strontium isotopes~~ Sr isotope composition: ^{87}Sr/^{86}Sr and $\delta^{88/86}$Sr

The Sr isotope composition of seawater is recorded at the time of formation of~~, for example,~~ carbonate skeletons of marine organisms ~~for example~~ (McArthur et al., 2001; Banner, 2004). The Sr isotope~~-~~composition of ocean water results from the mixing of several Sr sources

Formatted: English (United States)

Formatted: English (United States)

Formatted: Underline, English (United States)

Formatted: Underline

Formatted: Font: Not Italic

Formatted: English (United States)

with different isotopic signatures (McArthur et al., 2001; Banner, 2004). Terrigenous material of continental origin with ~~a high~~high ^{87}Sr/^{86}Sr ratios (~~currently the isotopic composition~~modern value of ~~the~~ continental runoff ~~is estimated to be~~of 0.7116; Palmer and ~~,~~ Edmond, 1989) is carried into ~~the~~ ocean basins by rivers, glaciers, and wind. During the weathering of mid-ocean ridge basalts and ~~the~~ halmyrolysis of ocean~~-~~ floor rocks, Sr with a low ^{87}Sr/^{86}Sr ratio enters the water (modern value of 0.7037; Palmer and ~~,~~ Edmond, 1989). The smallest sources of Sr are marine carbonates, which release upon recrystallization a part of the Sr held in the crystal lattice, which has an average isotopic ratio of 0.7084 (Holland, 1984; De Paolo, 1987; Davis et al., 2003; Banner, 2004). The modern global-ocean ~~value of~~ ^{87}Sr/^{86}Sr ratio ~~in the World Ocean~~ is 0.70917 (Burke et al., 1982; Faure, 1986; Hodell et al., 1989; Banner, 2004; McArthur et al., 2012, 2020).

~~The~~ A comparison of the Sr isotope composition of carbonate rocks with the LOWESS global ^{87}Sr/^{86}Sr variation curve (McArthur et al., 2001, 2012, 2020) makes it possible to determine the age of their formation. ~~At the same time, the~~The ratio of stable ^{88}Sr and ^{86}Sr ~~and ^{88}Sr~~ isotopes (defined as $\delta^{88/86}$Sr ~~via~~ with respect to NIST SRM-987 or $\delta^{88/86}$Sr) ~~in whole, depends on temperature of seawater and species~~ in marine carbonates generally depends on the $\delta^{88/86}$Sr value of seawater, which changes through time owing to variations in the same fluxes that control seawater $^{87/86}$Sr and the net carbonate flux from the ocean, as well as the degree of fractionation between seawater and carbonate, which depends on species and temperature (Rüggeberg et al., 2008; Krabbenhöft et al., 2010; Vollstaedt et al., 2014; Pearce et al., 2015; Paytan et al., 2021). In the modern ocean, $\delta^{88/86}$Sr is 0.378‰ to ~~-~~0.402 ~~‰~~‰ (IAPSO standard seawater, http://georem.mpch-mainz.gwdg.de/sample_query.asp). ~~The mineral particles formed in water are characterized by the lower $\delta^{88/86}$Sr. Moreover, the minerals of chemogenic and biogenic origins can be distinguished by the degree of their stable Sr isotope fractionation (Fietzke and Eisenhauer, 2006; Fruchter et al., 2016). Besides this, the organism behaviour, in particular, the presence of absence of temperature dependence, varies for different species. Thus, belemnites and cold-water corals don't exhibit any temperature dependence (Rüggeberg et al., 2008; Vollstaedt et al., 2014), while $\delta^{88/86}$Sr in tropical corals increases with the temperature growth (Fietzke and Eisenhauer, 2006; Rüggeberg et al., 2008), and coccolithophores reveal the inverse temperature relationship (Stevenson et al., 2014). In our work, warm-water species corals had replaced as the dominant species by Larger benthic foraminifera (LBF) and coralline algal, that associated with changes in water depth and temperature. Therefore, we expect that $\delta^{88/86}$Sr will change with this species transition. However, in this case, it is practically impossible to predict the direction of change (whether $\delta^{88/86}$Sr will increase or decrease).~~ Minerals such as carbonate formed in seawater are generally characterized by lower $\delta^{88/86}$Sr than seawater because

Formatted: English (United States)

Formatted: English (United States)

Formatted: English (United States)

Formatted: English (United States)

of seawater–mineral fractionation. Moreover, minerals of chemogenic and biogenic origins can be distinguished by the degree of their stable Sr isotope fractionation (Fietzke and Eisenhauer, 2006; Fruchter et al., 2016; AlKhatib and Eisenhauer, 2017; Müller et al., 2018), which depends on temperature and species. Thus, belemnites and cold-water corals do not exhibit temperature dependence of their stable Sr isotope fractionation (Rüggeberg et al., 2008; Vollstaedt et al., 2014), whereas $\delta^{88/86}Sr$ in tropical corals increases with sea surface temperature (Fietzke and Eisenhauer, 2006; Rüggeberg et al., 2008), and coccolithophores show an inverse temperature relationship (Stevenson et al., 2014). In our study of Koko Guyot, warm-water corals were replaced over time by deeper-water LBF and coralline algae In our study of Koko Guyot, warm-water corals were replaced over time by deeper-water LBF and coralline algae. Therefore, we expect that $\delta^{88/86}Sr$ will change over time in association with this species transition/replacement from warm/shallow to cold/deep types. However, in the present study, it is practically impossible to predict the direction of change (i.e., whether $\delta^{88/86}Sr$ will increase or decrease), due to there are many factors (including sea temperature, sea salinity, and skeleton/shell growth rates) that complicate the interpretation of $\delta^{88/86}Sr$ measurements.

~~The formation of~~ Koko Guyot ~~occurred about~~formed at *c.* -50 Ma (Jackson et al., 1980; Tarduno ~~,~~et al., 2003; Duncan and Keller, 2004), and this ~~is an~~provides a key datum ~~important date~~ for the ~~subsequent~~ discussion below~~s~~. The mean $^{87}Sr/^{86}Sr$ ratio of ~~the~~ echinoid spines analyzed in this study ~~are~~ is 0.70917 ± 0.00001, which corresponds to the modern isotopic water composition. ~~Taking into account the error of the isotope curve, we can assert that the age of these echinoids is comprised between 50.000 years ago and the present (Fig. 4A).~~ Taking into account the errors associated with the LOWESS global $^{87}Sr/^{86}Sr$ variation curve (McArthur et al., 2001, 2012, 2020) we infer that the age of these echinoids is between 50 ka and the present (Fig. 4A). The youngest sample of ~~the~~ unaltered limestones used for isotope stratigraphy ~~was~~ is LV86-8-4, which ~~formed~~ yielded an age of 15.30 ± 0.15 Ma (Langhian, middle Miocene). Limestone sample LV86-9-1 ~~limestone~~ was formed at 18.20 ± 0.15 Ma, and LV86-9-4 at 19.07 ± 0.03 Ma (Burdigalian, early Miocene). ~~The~~ Sample LV86-9-9, which is composed of the ~~sample with the~~ remains of Merulinidae corals, formed at the Aquitanian–Burdigalian (early Miocene) boundary (20.1 ± 0.3 Ma), ~~while~~ whereas the limestone sample ~~older~~ LV86-9-2 ~~limestone sample~~ containing *Astrea* cf. *annuligera* is Aquitanian in age (21.65 ± 0.3 Ma). The oldest studied sample ~~studied~~, LV86-9-6, is Chattian (Oligocene) in age (25.55 ± 0.45 Ma). Samples LV86-9-2, LV86-9-6, and LV86-9-9, ~~yelding~~ bearing *Spiroclypeus tidoenganensis* and *Heterostegina* cf. *assilinoides*, are latest Chattian (Oligocene) to Aquitanian in age. *Spiroclypeus tidoenganensis* has ~~been already~~previously been recognized from the upper Oligocene of Koko Guyot (Hottinger, 1975). Although this species has been reported ~~in~~ from coeval deposits ~~from~~

Formatted: English (United States)

Formatted: English (United States)

Formatted: English (United States)

in Saipan (Hanzawa, 1957), ~~one cannot rule out~~ its Aquitanian age is firm (e.g., Hottinger, 1975; Lunt and Allan, 2007). ~~These samples have also mean ages based on Sr-isotopes of 21.65, 25.55 and 20.1 Ma, consistent with the Chattian–Aquitanian age assessed by the larger foraminiferal species. Comparison with the curve of ^{87}Sr/^{86}Sr variations for the altered samples LV86-4, LV86-8-2, and LV86-8-3 gives the following ages: 6.7±0.3, 26.3±0.5, and 29.2±0.5 Ma, respectively. Interestingly, the last two ages are very close to the time of the LV86-9-6 deposition, and the samples LV86-8-2 and LV86-8-3 may have retained an almost initial composition.~~ The three limestone samples LV86-9-2, LV86-9-6, and LV86-9-9 have mean ages of 21.65, 25.55, and 20.10 Ma (based on Sr isotopes), respectively, consistent with the Chattian–Aquitanian age inferred from LBF species. A comparison with the LOWESS 3 global ^{87}Sr/^{86}Sr variation curve (McArthur et al., 2001, 2012) for altered samples LV86-4, LV86-8-2, and LV86-8-3 gives ages of 6.7 ± 0.3, 26.3 ± 0.5, and 29.2 ± 0.5 Ma, respectively. The last two ages are close to the age of LV86-9-6, suggesting that samples LV86-8-2 and LV86-8-3 may have approximately retained their initial compositions.

Formatted: English (United States)

~~During the last 35 Ma the δ$^{88/86}$Sr of sea water decreased from 0.38 to 0.30‰ (within ±0.02‰ analytical error) from 30 to 20 Ma (Paytan et al., 2021; Fig. 4B). Five samples are in this time period. Two of them (Lv 86-8-2, Lv 86-8-3) were probably subject to secondary alterations. It is believed (Voigt et al., 2015) that the δ$^{88/86}$Sr values are more variable in secondary processes. Therefore, for further discussion, we use only those samples that are the least modified. The δ$^{88/86}$Sr value of these samples varies from 0.26 to 0.37‰. Within the margin of error (±0.09‰), the results obtained intersect the line of the isotopic composition of water proposed by Paytan et al., (2021). The stable Sr isotope composition of younger samples from 20 to 15 Ma (LV86-8-4, LV86-9-1, LV86-9-4) comprising cold-water sea species and barren in corals, is rather uniform and average varies near 0.10±0.03‰. The change in the temperature and light regime led to the biocommunity alteration, in our case, reef benthic assemblages were replaced as the dominant species to larger foraminiferal species. We suppose that it is expressed in the dramatic decrease of δ$^{88/86}$Sr (Fig. 4). Biocommunity alteration to much more cool water resistance can be correlated with the bottom subsidence rate and guyot migration to higher latitudes (Wilson, 1963; Clague and Dalrymple, 1987; Tarduno et al., 2003; Clague et al., 2010). The δ$^{88/86}$Sr values of modern echinoids are also less then δ$^{88/86}$Sr curve. It is probably that Sr isotope fractionation between cold water species and water is much stronger than between warm water species and surrounding water. However, the last statement requires additional research and is beyond the scope of this study.~~ From 30 to 20 Ma, the δ$^{88/86}$Sr of seawater decreased from 0.38‰ to 0.30‰ (within ±0.02‰ analytical error) (Paytan et al., 2021; Fig. 4B). Five of the studied samples have ages within this time interval. Two of these samples (LV86-8-2 and LV86-

8-3) have probably been affected by diagenetic alteration. Because diagenetic processes have been shown to alter the initial $\delta^{88/86}$Sr of carbonates (Voigt et al., 2015), we use only the three least modified samples as a basis for our discussion. The $\delta^{88/86}$Sr value of these samples varies from 0.26‰ to 0.37‰. Within the margin of error (±0.09‰), the results obtained intersect the line indicating the isotopic composition of seawater proposed by Paytan et al. (2021). The stable Sr isotope composition of younger samples from 20 to 15 Ma (LV86-8-4, LV86-9-1, and LV86-9-4) comprising cold-water sea species and lacking corals is rather uniform, with the mean $\delta^{88/86}$Sr varying within 0.10‰ ± 0.03‰. These values are much lower than the isotope curve proposed by Paytan et al. (2021) (Fig. 4B). The $\delta^{88/86}$Sr values of modern echinoids are also lower than (although within measurement errors of) the $\delta^{88/86}$Sr curve.

It has been shown that carbonates have lower $\delta^{88/86}$ Sr values than the sedimentation medium, and the difference can be more than 0.1‰ (Raddatz et al., 2013, Vollstaedt et al., 2014). Kisakürek et al. (2011) and Böhm et al. (2013) explained this disparity by calcification in a largely open system at high precipitation rates. The shift to a benthic community that is more resistant to colder water can be correlated with bottom subsidence and guyot migration to higher latitudes (Wilson, 1963; Clague and Dalrymple, 1987; Tarduno et al., 2003; Clague et al., 2010). The change in temperature and light regime at Koko Guyot as it subsided and migrated to higher latitudes led to a change in the benthic community as reef benthic assemblages were replaced by those dominated by LBF (and coralline algae). The change in temperature and light regime at Koko Guyot as it subsided and migrated to higher latitudes led to a change in the benthic community as reef assemblages were replaced by those dominated by LBF and coralline algae. We presume that this change in benthic community is recorded as a sharp decrease in $\delta^{88/86}$Sr valuesi in our samples compared to sea water (Fig. 4B) without major changes in seawater $\delta^{88/86}$Sr values It is probable that Sr isotope fractionation between cold-water species and ambient seawater is much stronger than that between warm-water species and ambient seawater. However, we cannot take into account temperature and depth changes in this paper.

4.2. Rate of subsidence of Koko Guyot and its variation over time~~Subsidence rates~~

Grigg (1988) identified corals *Favites* sp., *Platygyra* sp., *Psammocora* (*Stephanaria*) sp., and *Seriatopora* sp. from Koko Seamount, the ages of which ranged from 30.5 to 24.7 Ma, ~~via~~ as determined using Sr isotope stratigraphy. Clague et al. (2010) obtained ages for corals ranging from 50 to 27 Ma, ~~whereas~~ compared with 16 Ma for LBF ~~16 Ma~~, on the basis of which those authors~~.~~ ~~Discussing these data, Clague et al. (2010)~~ calculated the subsidence rate of the volcano ~~to be~~as 0.012 ± 0.003 mm/yr. ~~Previously~~ Davies et al. (1972) ~~based on~~used water depth, guyot

Formatted: English (United States)

Formatted: English (United States)

Formatted: English (United States)

Formatted: Underline

structure, and the age and species composition of corals to~~,~~ estimate~~d~~ the subsidence rate of Koko Guyot ~~at~~ as ~~42 m/Ma or~~ 0.042 mm/yr throughout the existence of the guyot.

Our method of estimation~~estimation~~ of subsidence rates for Koko Guyot ~~subsidence rate~~ ~~follows these~~incorporated the following assumptions: (1) reef formation slowed ~~down~~ and then stopped ~~due~~ owing to submersion below the euphotic zone, ~~the~~ which is the lower depth limit of coral and algal growth;~~,~~ (2) the identified fossil benthic assemblage from the guyot~~'s~~ plateau lived in optimal ~~conditions of~~ depth (i.e., 0–30 m) and temperature (average winter water temperature >18 °C) conditions for reef growth (Veron, 1995);~~,~~ and (3) later benthic communities, devoid of reef corals, lived at greater water depths >30 m. Warm-water corals grow at a certain depth, no more than 30 m (Veron, 1995). As the seafloor subsides and relative sea-level rise resultantly occurs, ~~,~~the reef ~~buildup grows~~builds up vertically to retain a ~~the~~ ~~"comfortable life"~~ zone of maximum favorability for coral existence~~s~~. We took the maximum water depth of this zone for ~~such~~ corals in this study ~~at~~ as 30 m. We also ~~decided~~ assumed that the formation of the carbonate skeleton occurred~~s~~ under normal conditions. With ~~the~~ gradual subsidence of the seafloor, we assumed that the reef of Koko Guyot was able to keep up with sea~~-~~level rise ~~as~~ so long as the seafloor was within the euphotic zone. As the rate of sinking increased~~s~~, new colonies ~~will~~ would have formed ~~faster~~ more quickly to grow to a ~~comfortable~~ favorable depth (maximum 30 m). ~~Thus, samples with a small difference in age will occur more often. Proceeding from the sample ages obtained, we plotted the curve of the coral age *versus* the age difference (Fig. 5). It can be seen from the graph that the age difference between the samples at the early stage of "guyot life" is smaller, and this difference increases with age. This suggests that the rate of reef growth, or volcano's subsidence, was irregular.~~ With a high subsidence rate, the coral growth rate will also be faster. The «new» corals will record the «new» isotopic composition of water. Thus, samples with a small difference in age will occur more often. Thus, we have described our «model object» and proceed to the calculations.

We took all age estimates (Grigg, 1988; Clague et al., 2010; this work), ranked them from ~~minimum~~ youngest to ~~maximum~~oldest, and calculated the difference between each successive age (~~difference ranged~~which ranged from ~~from~~ 0 to 2 Myr), thus ~~. As a result, we~~ obtaining~~ed~~ 26 ~~points~~ datapoints (Table 5 and~~,~~ Fig. 5). Figure 5 shows that the age difference between the samples during the early stage of guyot evolution is small and that this difference increases with Koko Guyot age. The pattern of data in Fig. 5 suggests that the rate of reef growth (or of the guyot's subsidence) varied over time. The age difference ~~over~~ for the period 30–25 Ma is smaller than that ~~during~~ for ~~the period~~ 25–15 Ma, suggesting that the reef grew ~~faster~~ more quickly during the older period. The age of the youngest identified coral specimen is 20.1 ±~~–~~ 0.3 Ma (LV86-9-9). This sample may~~,~~ therefore~~,~~ mark the ~~last~~ final episode of active reef growth, after

Formatted: English (United States)

Formatted: English (United States)

Formatted: English (United States)

Formatted: English (United States)

Formatted: English (United States)

Formatted: English (United States)

Formatted: English (United States)

Formatted: English (United States)

Formatted: English (United States)

Formatted: English (United States)

Formatted: English (United States)

Formatted: English (United States)

Formatted: English (United States)

Formatted: English (United States)

Formatted: English (United States)

which the platform ~~was more deepened~~deepened to a position ~~and located~~ below the euphotic zone~~ where corals can thrive due to the subsidence of the guyot~~ (Wilson, 1963; Clague and Dalrymple, 1987; Tarduno et al., 2003; Clague et al., 2010). ~~Moreover, we~~We also sampled a coralline algal crust dated at 15 Ma (LV86-8-4). The sample was collected from a depth of 1~~.~~458 m, where it ~~laid~~ was located in a soft (unconsolidated) substrate. ~~It~~ This sample most likely slid down the slope from the nearest plateau, whose current top ~~is today at~~height is at 350 m water depth. Assuming a maximum water depth of 120 m for the living coralline algae and 30 m for the living youngest zooxanthellate corals sampled (Clague et al., 2010), we ~~have~~ calculated ~~that~~ the following: (1) ~~F~~from ~~or the last~~ 15 Ma to the present, Koko Guyot subsided at a ~~speed~~ rate of (350 – ~~–~~ 120)/15.3 = 15.0 m/Myr, that is, ~~(i.e.,~~ 0.015 ± ~~–~~ 0.002 mm/yr~~);~~ and (2) ~~in~~ during the period from 20 to 15 Ma, the ~~average~~ mean subsidence rate was (120 – ~~–~~ 30)/(20.1 – ~~–~~ 15.3) ~~=~~ = 18.8 m/Myr, that is, 0.019 ± ~~–~~ 0.003 mm/yr. ~~Previous studies~~A previous study ~~suggest~~ has suggested that the ~~very first~~initial shallow-water sediments formed ~~in~~ during the period from ~~from~~ 49.7 ~~to~~ 43.5 Ma, ~~which was found~~as identified in the ODP Site 1206 (Fig. 1) core recovered at 1500 m water depth (Shipboard Scientific Party, 2002). The bottom of this layer was 57 m from the top of the column (Shipboard Scientific Party, 2002; Tarduno et al., 2003). Thus, ~~if we~~ applying our calculation method, the subsidence rate ~~in~~ during the first tens of million years (from 49.7 to 43.5 Ma) is estimated a~~s~~t ~~approximately~~ 0.046 ± ~~–~~ 0.005 mm/yr [using ~~(as the average of 49.7 and 43.5 Ma is 46.6 Ma, we calculate the subsidence rate as follows:~~ (1500 + 57 – ~~–~~ 350)/(46.6 – ~~–~~ 20.1) = 46.2~~)~~ m/Myr or 0.046 ± 0.005 mm/yr, where 46.6 Ma is the mean of 49.7 and 43.5 Ma] (Fig. 6), which ~~was~~ is close to the rate reported by Davies et al. (1972). ~~Our calculations showed that the~~ Our calculated average subsidence rate ~~was~~ is ~~slightly~~ higher than that ~~suggested~~ estimated by Clague et al. (2010) of~~, i.e.~~ 0.008–0.012 mm/yr~~)~~ ~~over~~ since~~last~~ 23 Ma~~yr~~. ~~Our~~ However, our results are consistent with ~~other observations that~~the observation that the subsidence rate of the ocean floor decreases as the age of the ocean crust increases (~~for example,~~e.g., Sclater et al., 1980; Marty and Cazenave, 1989; Stein and Stein, 1992). This process represents ~~the~~ seafloor flattening, meaning that old seafloor is shallower than that predicted by the "root-t" model (i.e., a linear increase in ocean depth with increasing crustal age; Parsons and Sclater, 1977; Hillier, 2010).

5. Conclusions

~~The study of Sr isotope composition showed that the least altered limestones containing the fragments of reef corals were formed in the early Miocene. No coral fragments were found in~~

Formatted: Underline, English (United States)
Formatted: English (United States)
Formatted: English (United States)
Formatted: English (United States)
Formatted: English (United States)
Formatted: English (United States)
Formatted: English (United States)
Formatted: English (United States)
Formatted: English (United States)
Formatted: No underline, English (United States)
Formatted: English (United States)
Formatted: English (United States)
Formatted: English (United States)
Formatted: English (United States)
Formatted: English (United States)
Formatted: English (United States)
Formatted: English (United States)
Formatted: English (United States)
Formatted: English (United States)
Formatted: English (United States)

~~older samples (Late Oligocene). A study of the distribution of stable strontium isotopes in warm-water marine organisms and cold-water ones showed that the fractionation of stable strontium isotopes between cold-water species and water is probably higher than between warm-water ones and water.~~ We investigated the Sr isotope compositions of Oligocene–Miocene coral reef limestone from Koko Guyot in the southern Emperor Seamount Chain to assess the dynamics of the subsidence of this guyot. Our study of Sr isotope compositions ($^{87}Sr/^{86}Sr$) showed that the least altered limestones containing fragments of reef corals were formed during the early Miocene. No coral fragments were found in older samples (late Oligocene). Analysis of the distribution of stable Sr isotopes ($\delta^{88/86}Sr$) in warm-water sediments showed a low degree of fractionation compared with seawater. The $\delta^{88/86}Sr$ values of cold-water species, which replaced warm-water species at around 20 Ma, differ significantly from the seawater $\delta^{88/86}Sr$ variation curve estimated by Paytan et al. (2021).

~~Using several independent methods, we confirm the change in environmental parameters and determine the time limit of this change about 20 Ma. The same boundary corresponds to a change in the rate of subsidence. From about 49–44 Ma to 20 Ma the subsidence rate of Koko Guyot was 0.046±0.005 mm/yr. The~~ ~~$\delta^{88/86}Sr$~~ ~~values of coral samples, that formed 25–20 Ma, varies from 0.26 to 0.37 (±0.09)‰ and these values are consistent with the variation curve proposed by Paytan et al., (2021). At the lower limit of this period, the biocommunity was re-adjusted due to the fact that the surrounding waters became colder. Warm water corals disappeared and were replaced by Larger benthic foraminifera and coralline algal. From 20 to 15 Ma ago, the subsidence rate was lower more than twice, 0.019±0.003 mm/yr. The~~ ~~$\delta^{88/86}Sr$~~ ~~values of this samples are about 0.10‰. Finally, in the last 15 Ma the volcanic structure has been subsided at a rate of 0.015±0.002 mm/yr. The data obtained refine the existing models of subsidence of the Pacific crust. Understanding the differential rate of subsidence is important insofar as it supports the model of ocean floor cooling after the Pacific plate passed over the stationary mantle hotspot, which may be particularly important insofar as the seamount sits at the juncture of plate rotation as seen from the different trajectory of the Emperor and Hawaiian chains.~~ Using several independent methods, we confirmed a change in environmental parameters at around 20 Ma. This timing also corresponds to a change in the rate of subsidence. From 49–44 to 20 Ma, the subsidence rate of Koko Guyot was 0.046 ± 0.005 mm/yr. The $\delta^{88/86}Sr$ values of coral samples that formed from 25 to 20 Ma vary from 0.26‰ to 0.37‰ (±0.09‰) and are consistent with the variation curve proposed by Paytan et al. (2021). At the ending of this period, the benthic community changed because of cooling ambient waters. Warm-water corals disappeared and were replaced by LBF and coralline algae. From 20 to 15 Ma, the subsidence rate was much lower at 0.019 ± 0.003 mm/yr. The $\delta^{88/86}Sr$ values for samples that formed during this period are ~0.10‰. Since 15 Ma, the volcanic structure has subsided at a rate of 0.015 ± 0.002 mm/yr. The data obtained in this study refine existing models of the crustal subsidence of the floor of the Pacific Ocean, which suggest a constant rate of seafloor subsidence. Understanding the changing rate of subsidence is important because it is related to the process of ocean-floor cooling after the Pacific Plate passed over the mantle Hawaiian hotspot.

Declaration of competing interests

Formatted: English (United States)

The authors declare that they have no known competing financial interests or personal relationships that could have appeared to influence the work reported in this paper.

Acknowledgments

The authors are grateful to Tatyana Nikolaevna Dautova (~~the~~ Head of the 86th voyage of the ~~R/V~~research vessel “Akademik M.A. Lavrentiev”) ~~Tatyana Nikolaevna Dautova~~ and to A.V. Zhirmunsky (National Scientific Centre of Marine Biology FEB RAS ~~(~~Vladivostok) for organizing the work; and~~,~~ to the members of the Deepwater Equipment Department of A.V. Zhirmunsky National Scientific Centre of Marine Biology, Far Eastern Branch, Russian Academy of Sciences (NSCMB FEB RAS)~~),~~ and Alexei Mikhailovich Asavin for their help with rock sampling. The authors ~~wish to express their gratitude to~~thank Aleksey Kotov for his assistance with carbonate rock sample analyses~~s~~.

Formatted: English (United States)

~~We thank the anonymous reviewers for the important comments and constructive suggestions, which improved the quality of the manuscript.~~ We thank Editor-in-Chief of Marine Geology Dr. Adina Paytan and anonymous reviewers for their valuable comments and suggestions, which improved the quality of the manuscript.

Participation in the 86th voyage of the R/V “Akademik M.A. Lavrentiev” was made possible ~~due~~ owing to a state assignment of the FEGI FEB RAS (state registration number AAAA-A17-117092750071-2). – The reequipment and comprehensive development of the “Geoanalitik” shared research facilities of the IGG UB RAS was~~is~~ financially supported by ~~the~~ a grant ~~of~~ by the Ministry of Science and Higher Education of the Russian Federation for 2021–2023 (Agreement No. 075-15-2021-680). Chemical and isotopic investigations were ~~carried out~~conducted in the Geoanalitik Center for Collective Use of the IGG UB RAS as ~~a~~ part of the state assignments of the GEOCHI RAS ~~(state assignment No. XXX)~~ and IGG UB RAS (state registration number AAAA-A18-118053090045-8).

Formatted: English (United States)

Formatted: English (United States)

Formatted: English (United States)

Formatted: English (United States)

~~The authors are grateful to Editor-in-Chief of Marine Geology Dr. Adina Paytan and reviewers who made great job for improving the manuscript.~~

Data availability

All data ~~is~~ are provided in attached files and at~~on~~ https://doi.org/10.5281/zenodo.6330970.

References

AlKhatib, M., Eisenhauer, A., 2017. Calcium and strontium isotope fractionation during precipitation from aqueous solutions as a function of temperature and reaction rate; II. Aragonite. Geochim. Cosmochim. Acta, 209, 320-342. https://doi.org/10.1016/j.gca.2017.04.012

Banner, J.L., 2004. Radiogenic isotopes: systematics and applications to earth surface processes and chemical stratigraphy. Earth-Sci. Rev. 65, 141–194. https://doi.org/10.1016/S0012-8252(03)00086-2

Böhm, F., Eisenhauer, A., Tang, J., Dietzel, M., Krabbenhöft, A., Kisakürek, B., Horn, C. 2012. Strontium isotope fractionation of planktic foraminifera and inorganic calcite. Geochim. Cosmochim. Acta, 93, 300-314. https://doi.org/10.1016/j.gca.2012.04.038

Burke, W.H., Denison, R.E., Hetherington, E.A., Koepnick, R.B., Nelson, H.F., Otto, J.B., 1982. Variation of seawater $^{87}Sr/^{86}Sr$ throughout Phanerozoic time. Geology 10, 516–519.

Certificate of analysis IAG / CGL 020 ML-3 (Limestone), 2015. International Association of Geoanalysts http://iageo.com/wp-content/uploads/2020/08/ML-3-certificate.pdf (accept 21.02.2022)

Charlier, B.L.A., Nowell, G.M., Parkinson, I.J., Kelley, S.P., Pearson, D.G., Burton, K.W., 2012. High temperature strontium stable isotope behaviour in the early solar system and planetary bodies. Earth Planet Sci Lett 329, 31–40.

Clague, D.A., Braga, J.C., Bassi, D., Fullagar, P.D., Renema, W., Webster, J.M., 2010. The maximum age of Hawaiian terrestrial lineages: geological constraints from Kōko Seamount. J. Biogeogr. 37, 1022–1033. https://doi.org/10.1111/j.1365-2699.2009.02235.x

Clague, D.A., Dalrymple, G.B., 1987. The Hawaiian-Emperor volcanic chain. part I. Geologic evolution. Volcanism in Hawaii. 1, 5–54.

Dalrymple, G.B., Clague, D.A., 1976. Age of the Hawaiian–Emperor bend. Earth Plan. Sci. Lett. 31, 313–329.

Davies, T.A., Wilde, P., Clague, D.A., 1972. Koko Seamount: A major guyot at the southern end of the Emperor Seamounts. Mar. Geol. 13, 311–321.

Davis, A.C., Bickle, M.J., Teagle, D.A.H. Imbalance in the oceanic strontium budget. Earth Planet. Sci. Lett., 2003. 211, 173– 187.

DePaolo, D.J., 1987. Correlating rocks with strontium isotopes. Geotimes 32 (12), 16–18.

Duncan, R.A., Keller, R.A., 2004. Radiometric ages for basement rocks from the Emperor Seamounts, ODP Leg 197. Geochem. Geophys. Geosyst., 5, Q08L03. doi:10.1029/2004GC000704

Faure, G., 1986. Principles of Isotope Geology. 2nd ed. New York, Willey et Sons.

Fietzke, J., Eisenhauer, A., 2006. Determination of temperature-dependent stable strontium isotope (^{88}Sr/^{86}Sr) fractionation via bracketing standard MC-ICP-MS. Geochem. Geophys. Geosyst. 7, Q08009, doi:10.1029/2006GC001243

Fruchter, N., Eisenhauer, A., Dietzel, M., Fietzke, J., Böhm, F., Montagna, P., Stein, M., Lazar, B., Rodolfo-Metalpa, R., Erez, J., 2016. 88Sr/86Sr fractionation in inorganic aragonite and in corals. Geochimica et Cosmochimica Acta 178, 268-280, https://doi.org/10.1016/j.gca.2016.01.039

GeoReM database http://georem.mpch-mainz.gwdg.de/ (accept 21.02.2022)

Greene, H.G., Clague, D.A., Dalrymple, G.B., 1980. Seismic stratigraphy and vertical tectonics of the Emperor Seamounts. DSDP Leg 55. Initial reports of the Deep Sea Drilling Project. Wash. (D.C.), US Gov. print, off. 55, 759–788.

Grigg, R.W., 1988. Paleoceanography of coral reefs in the Hawaiian-Emperor Chain. Science 240, 1737–1743.

Hanzawa, S. 1957. Cenozoic foraminifera of Micronesia. Geol. Soc. Am., Mem. 66, 163 pp.

Henson, F.R.S., 1937. Larger foraminifera from Aintab, Turkish Syria. Eclog. Geol. Helv. 30, 45-57.

Hillier, J.K., 2010. Subsidence of “normal” seafloor: Observations do indicate “flattening”. J. Geophys. Res. Solid Earth 115(B3). https://doi.org/10.1029/2008JB005994

Hodell, D.A., Mueller, P.A., McKenzie, J.A., Mead, G.A., 1989. Strontium isotope stratigraphy and geochemistry of the late Neogene ocean. Earth Planet. Sci. Lett. 92, 165–178.

Holland, H.D., 1984, The Chemical Evolution of the Atmosphere and Oceans. Princeton University Press, Princeton, NJ, pp. 582.

Hottinger, L. 1975. Late Oligocene larger foraminifera from Koko Guyot, site 309. Initial Reports of the Deep Sea Drilling Project, 32, 825–826.

Jackson, E. D., Koisumi, I., Dalrymple, G., Clague, D., Kirkpatrick, R., Greene, H., 1980. Introduction and summary of results from DSDP Leg 55, the Hawaiian–Emperor hot-spot experiment. Initial reports of the deep sea drilling project, 55, 5–31.

Jochum, K.P., Garbe-Schonberg, D., Veter, M., Stoll, B., Weis, U., Weber, M., Lugli, F., Jentzen, A., Schiebel, R., Wassenburg, J.A., Jacob, D.E., Haug, G.H., 2019. Nano-powdered calcium carbonate reference materials: significant progress for microanalysis? Geostand. Geoanal. Res. 43: 595-609. https://doi.org/10.1111/ggr.12292

Keller, R.A., Fisk, M.R., White, W.M., 2000. Isotopic evidence for Late Cretaceous plume–ridge interaction at the Hawaiian hotspot. Nature 405(6787), 673–676. doi:10.1038/35015057

Kisakürek, B., Eisenhauer, A., Böhm, F., Hathorne, E.C., Erez, J., 2011. Controls on calcium isotope fractionation in cultured planktic foraminifera, *Globigerinoides ruber* and *Globigerinella siphonifera*.– Geochim. Cosmochim. Acta, 75, 427-443. https://doi.org/10.1016/j.gca.2010.10.015

Krabbenhöft, A., Eisenhauer, A., Böhm, F., Vollstaedt, H., Fietzke, J., Liebetrau, V., Augustin, N., Peucker-Ehrenbrink, B., Müller, M.N., Horn, C., Hansen, B.T., Nolte, N., Wallmann, K., 2010. Constraining the marine strontium budget with natural strontium isotope fractionations (87Sr/86Sr∗, δ88/86Sr) of carbonates, hydrothermal solutions and river waters. Geochim. Cosmochim. Acta 74 (14), 4097-4109. https://doi.org/10.1016/j.gca.2010.04.009

Krabbenhoft, A., Fietzke, J., Eisenhauer, A., Liebetrau, V., Bohm, F., Vollstaedt, H., 2009. Determination of radiogenic and stable strontium isotope ratios (87Sr/86Sr, δ88/86Sr) by thermal ionization mass spectrometry applying an 87Sr/84Sr double spike. J Anal At Spectrom 24, 1267–1271

Kuznetsov, A.B., Gorokhov, I.M., Semikhatov, M.A., 2018. Strontium isotope stratigraphy: Principles and State of the Art. Strat. Geol. Correl. 26, 367–386. https://doi.org/10.1134/S0869593818040056

Larson, R.L., Moberly, R., Bukry, D., Foreman, H.P., Gardner, J.V., Keene, J.B., Lancelot, Y., Luterbacher, H., Marshall, M.C., Matter, A., 1975. Site 308: Koko guyot. Site 309: Koko guyot. Initial reports of the Deep Sea Drilling Project. Wash. (D.C.): US Gov. print, off. 32, 215–231.

Lunt, P., Allan, T. 2004. Larger foraminifera in Indonesian biostratigraphy, calibrated to isotopic dating. Geological Research Development Centre Museum, Workshop on Micropalaeontology, Bandung, 109 pp.

Ma, J.L., Wei, G.J., Liu, Y., Ren, Z.Y., Xu, Y.G., Yang, Y.H., 2013. Precise measurement of stable ($\delta^{88/86}$Sr) and radiogenic (^{87}Sr/^{86}Sr) strontium isotope ratios in geological standard reference materials using MC-ICP-MS. Chinese Science Bulletin 58, 3111–3118.

Marty, J.C., Cazenave, A., 1989. Regional variations in subsidence rate of oceanic plates: a global analysis. Earth Plan. Sci. Let., 94 (3–4), 301-315, https://doi.org/10.1016/0012-821X(89)90148-9

McArthur, J.M., Howarth, R.J., Shields, G.A., 2012. Strontium isotope stratigraphy. The Geologic Time Scale 1, 127–144. DOI: 10.1016/B978-0-444-59425-9.00007-X

McArthur, J.M., Howarth, R.J., Shields, G.A., Zhou, Y., 2020. Chapter 7. Strontium Isotope Stratigraphy, in Gradstein, F.M., Ogg, J.G., Schmitz, M.D., Ogg, G.M. (Eds), Geologic Time Scale 2020, Elsevier, pp. 211–238, https://doi.org/10.1016/B978-0-12-824360-2.00007-3

McArthur, M., Howaith, R.J., Bailey, T.R., 2001. Strontium isotope stratigraphy: LOWESS Version 3: Best Fit to the Marine Sr-Isotope Curve for 0-509 Ma and Accompanying Look-up Table for Deriving Numerical Age. J. Geol. 109, 155–170. https://doi.org/10.1086/319243

Moynier, F., Agranier, A., Hezel, D.C., Bouvier, A., 2010. Sr stable isotope composition of Earth, the Moon, Mars, Vesta and meteorites. Earth Planet Sci Lett 300, 359–366

Milne Edwards, H., Haime, J., 1848. Recherches sur les polypiers. Mémoire 4. Monographie des Astréides (1) (suite). Annales des Sciences Naturelles, Zoologie, Series 3. 12, 3, 95-197.

Müller, M.N., Krabbenhöft, A., Vollstaedt., H, Brandini, F.P., Eisenhauer, A., 2018. Stable isotope fractionation of strontium in coccolithophore calcite: Influence of temperature and carbonate chemistry. Geobiology, 16, 297– 306. https://doi.org/10.1111/gbi.12276

Palmer, M.R., 1985. Rare earth elements in foraminifera tests. Earth Planet. Sci. Lett. 73(2-4), 285–298. doi:10.1016/0012-821x(85)90077-9

Palmer, M.R., Edmond, J.M., 1989. The strontium isotope budget of the modern ocean // Earth Planet. Sci. Letters 92, № 61, 11-26

Parsons, B., Sclater, J. G., 1977. An analysis of the variation of ocean floor bathymetry and heat flow with age. J. Geophys. Res. 82(5), 803–827.

Paytan, A., Griffith, E.M., Eisenhauer, A., Hain, M.P., Wallmann, K., Ridgwell, A., 2021. A 35-million-year record of seawater stable Sr isotopes reveals a fluctuating global carbon cycle. Science 371 (6536), 1346–1350. DOI: 10.1126/science.aaz9266

Pearce, C.R., Parkinson, I.J., Gaillardet, J., Charlier, B.L.A., Mokadem, F., Burton, K.W., 2015. Reassessing the stable ($\delta^{88/86}$Sr) and radiogenic (^{87}Sr/^{86}Sr) strontium isotopic composition of marine inputs. Geochim. Cosmochim. Acta 157, 125–146. https://doi.org/10.1016/j.gca.2015.02.029

Raddatz, J., Liebetrau, V., Rüggeberg, A., Hathorne, E., Krabbenhöft, A., Eisenhauer, A., Böhm, F., Vollstaedt, H., Fietzke, J., López Correa, M., Freiwald, A., Dullo, W.-Chr., 2013. Stable Sr-isotope, Sr/Ca, Mg/Ca, Li/Ca and Mg/Li ratios in the scleractinian cold-water coral Lophelia pertusa. Chem. Geol., 352, 143-152. https://doi.org/10.1016/j.chemgeo.2013.06.013

Rüggeberg, A., Fietzke, J., Liebetrau, V., Eisenhauer, A., Dullo, W.-C., Freiwald, A., 2008. Stable strontium isotopes ($\delta^{88/86}Sr$) in cold-water corals — A new proxy for reconstruction of intermediate ocean water temperatures. Earth Planet. Sci. Lett. 269 (3–4), 570–575. https://doi.org/10.1016/j.epsl.2008.03.002

Sawaki, Y., Ohno, T., Tahata, M., Komiya, T., Hirata, T., Maruyama, S., Windley, B.F., Han, J., Shu, D., Li, Y., 2010. The Ediacaran radiogenic Sr isotope excursion in the Doushantuo Formation in the Three Gorges area, South China. Precambrian Res. 176, 46–64. https://doi.org/10.1016/j.precamres.2009.10.006

Sclater, J. G., Jaupart, C., Galson, D., 1980. The heat flow through oceanic and continental crust and the heat loss of the Earth. Rev. Geoph. Space Physics, 18 (1), 269-311 https://doi.org/10.1029/RG018i001p00269

Shalev, N., Segal, I., Lazar, B., Gavrieli, I., Fietzke, J., Eisenhauer, A., Halicz, L., 2013. Precise determination of δ88/86Sr in natural samples by double-spike MC-ICP-MS and its TIMS verification. J Anal At Spectrom 28, 940–944.

Shipboard Scientific Party, 1975a. Site 308: Koko Seamount. Proceedings of the Deep Sea Drilling Project, Initial Reports, Vol. 32 (by R.L. Larson, R. Moberly, D. Bukry, H.P. Foreman, J.V. Gardner, J.B. Keene, Y. Lancelot, H. Luterbacher, M.C. Marshall and A. Matter), pp. 215–226. US Government Printing Office, Washington, DC.

Shipboard Scientific Party, 1975b. Site 309: Koko Seamount. Proceedings of the Deep Sea Drilling Project, Initial Reports, Vol. 32 (by R.L. Larson, R. Moberly, D. Bukry, H.P. Foreman, J.V. Gardner, J.B. Keene, Y. Lancelot, H. Luterbacher, M.C. Marshall and A. Matter), pp. 227–231. US Government Printing Office, Washington, DC.

Shipboard Scientific Party, 2002. Site 1206. Proceedings of the Ocean Drilling Program, Initial Reports, Vol. 197 (by J.A. Tarduno, R.A. Duncan and D.W. Scholl et al.), pp. 1–117. Ocean Drilling Program, College Station, TX.

Speijer, R. P., Pälike, H., Hollis, C. J., Hooker, J. J., Ogg, J. G., 2020. The Paleogene Period. In Geologic time scale 2020, 1087-1140. Elsevier.

Stein, C., Stein, S., 1992. A model for the global variation in oceanic depth and heat flow with lithospheric age. Nature 359, 123–129. https://doi.org/10.1038/359123a0

Stevenson, E.I., Hermoso, M., Rickaby, R.E.M., Tyler, J.J., Minoletti, F., Parkinson, I.J., Mokadem, F., Burton, K.W., 2014. Controls on stable strontium isotope fractionation in coccolithophores with implications for the marine Sr cycle. Geochim. Cosmochim. Acta 128, 225–235. https://doi.org/10.1016/j.gca.2013.11.043

Stoll H.M., Schrag D.P., 1998. Effects of Quaternary sea level cycles on strontium in seawater. Geochim. Cosmochim. Acta 62, 1107–1118. doi:10.1016/S0016-7037(98)00042-8

Tarduno, J.A., Duncan, R.A., Scholl, D.W., Cottrell, R.D., Steinberger, B., Thordarson, Th., Kerr, B.C., Neal, C.R., Frey, F.A., Torii, M., Carvallo, C., 2003. The Emperor Seamounts: southward motion of the Hawaiian Hotspot Plume in Earth's mantle. Science 301, 1064–1069. doi: 10.1126/science.1086442

Teng, F.-Z., Dauphas, N., Watkins, J.M., 2017. Non-Traditional Stable Isotopes: Retrospective and Prospective. Reviews in Mineralogy and Geochemistry 82(1), 1–26. doi: https://doi.org/10.2138/rmg.2017.82.1

Van der Vlerk, M., 1925. A study of Tertiary foraminifera from the "Tidoengsche Landen" (E Borneo). Nederl. Indie, Dienst Mijnb. Wetensch. Meded. 3, 13-38.

Veiser, J., 1983. Trace elements and isotopes in sedimentary carbonate. Carbonates: mineralogy and chemistry. Rev. Min. 11 (2), 260–299.

Veron, J.E.N., 1995. Corals in space and time: the biogeography and evolution of the Scleractinia. UNSW Press, Sydney NSW Australia, 321 pp.

Vishnevskaya, I.A., Okuneva, T.G., Kiseleva, D.V., Soloshenko, N.G., Streletskaya, M.V., Vosel, Yu.S., 2020. Trace element and Sr isotopic composition of bottom and near-surface oceanic water in the southern region of the Emperor Ridge. Mar. Chem. 224, 103808. https://doi.org/10.1016/j.marchem.2020.103808

Voigt, J., Hathorne, Ed C., Frank, M., Vollstaedt, H., Eisenhauer, A., 2015. Variability of carbonate diagenesis in equatorial Pacific sediments deduced from radiogenic and stable Sr isotopes. Geochim. Cosmochim. Acta 148, 360–377, http://dx.doi.org/10.1016/j.gca.2014.10.001

Vollstaedt H., Eisenhauer A., Wallmann K., Böhm F., Fietzke J., Liebetrau V., Krabbenhöft A., Farkaš J., Tomašových A., Raddatz J., Veizer J., 2014. The Phanerozoic δ88/86Sr record of seawater: New constraints on past changes in oceanic carbonate fluxes. Geochim. Cosmochim. Acta 128, 249–265, https://doi.org/10.1016/j.gca.2013.10.006

Wheeler, C.W., Aharon, P., 1991. Mid-oceanic carbonate platforms as oceanic dipsticks: examples from the Pacific. Coral Reefs 10, 101–114.

Wilson, J.T., 1963. A possible origin of the Hawaiian Islands. Canadian J. Phys. 41, 863–870.

Figure and table captions

Fig. 1. (A) ~~A,~~ G~~g~~eographic map of the Hawaiian–Emperor bend. (B)~~B,~~ Bathymetric map of Koko Guyot~~ bathymetric map~~. P~~, p~~oints represent sampling sites for dives 4, 8, 9, and 16. Deep Sea Drilling Project sites 308 and 309 and Ocean Drilling Program Site 1206 are shown by value. The s~~S~~ource of the bathymetric map is http://earthref.org.

Fig. 2. Photographs of s~~S~~ampling conducted by a Comanche remotely operated underwater vehicle. ~~of the Comanche type:~~ (A) R~~r~~ock sampling ~~with a manipulator~~ from the plateau of the guyot using a manipulator (dive 9; sample Lv86-9-2);~~;~~ (B) ~~with~~ Sampling using a scoop net mounted on the manipulator (dive 9; sample Lv86-9 echinoid).

Fig. 3. (A)~~A,~~ M~~m~~odern octocoral of the ~~family~~ Isididae family (sample Coral). (B)~~,~~ E~~e~~chinoderm spines (Cidaroida; sample LV86-9, echinoid). (C–D) ~~-~~L~~l~~arger~~-~~foraminiferal packstone with *Spiroclypeus tidoenganensis* (*St*) and *Heterostegina* cf. *assilinoides* (*Ha*) (samples Lv86-9-2 and~~,~~ Lv86-9-6). (E)~~,~~ R~~r~~eef coral *Astrea* cf. *annuligera* (sample Lv86-9-2; i, thickened costo-septum; ii, paliform lobe). (F–G)~~,~~ B~~b~~ioclastic packstone showing (F) the encrusting coralline *Lithoporella* sp. with two uniporate conceptacles (arrows; sample LV86-8-3; conc., conceptacle)~~,~~ and (G) bryozoans (bry) and coralline fragments (cor; sample LV86-9-4).

Fig. 4. Comparison of the Sr isotopic composition of the studied samples with (A) the r~~R~~adiogenic Sr isotope record (LOWESS 5;~~,~~ McArthur et al., 2012) and (B) a model of the stable Sr isotope record with ±~~–~~0.02‰ analytical uncertainty (gra~~e~~y area;~~,~~ Paytan et al., 2021) in the ocean. Crossed-out circles ~~are~~ represent data from diagenetically altered samples. E~~, e~~rror bars ~~at the level of~~are ±~~–~~0.09‰.

Fig. 5. Relationship between age and age difference between two consecutive ages for carbonate samples. The difference between the ages of ~~the~~ consecutive older samples is less than that of the younger ~~ones~~samples. This suggests that the rate of subsidence of the reef superstructure ~~in ancient times~~was initially high~~ was higher than afterwards~~and subsequently decreased (i.e., the subsidence rate was higher when the coral reef and the guyot were younger). Data from this

work (circles), Grigg (1988,~~;~~ diamonds), and Clague et al. (2010,~~;~~ squares) are plotted in the ~~graph~~figure.

Fig. 6. Schematic model for the vertical motion~~s~~ of Koko Guyot. The bold line in the graph shows the changing position of the summit of the volcano, which formed at 49–48 Ma (Jackson et al., 1980; Tarduno ~~,~~ et al., 2003; Duncan and Keller, 2004). The ~~numbers in the figure~~rates given in the figure indicate the subsidence rate, calculated ~~according to the assumptions adopted in the text~~using the method presented in Section 4.2.

Table 1. Coordinates and water depths of samples ~~analysed~~ analyzed in this study, and seawater temperature and salinity at the sampling sites.
T, water temperature; S, salinity; Coral, sample of modern ~~Isididae~~ isididae coral; echinoid, sample of echinoid spines.

Table 2. Lithology and biotic components of the studied Koko Guyot carbonate samples.

Table 3. Trace-~~-~~element contents and calculated Fe/Sr and Mn/Sr ratios ~~in~~ of the studied carbonates. ~~The a~~Analys~~e~~is ~~was~~ were ~~carried out by~~performed using ~~the~~ ICP-~~–~~AES. C~~, and the c~~ontents are given in ppm.

Table 4. Strontium isotope compositions and ages according to LOWESS 5 (McArthur et al., 2001, 2012).

Table 5. Strontium isotope ages of samples from the present study and previous studies (blue, Grigg, 1988; yellow, Tarduno et al., 2003; green, Clague et al., 2010; white, this ~~work~~study) used to calculate age differences between consecutive samples.~~.~~

Formatted: English (United States)
Formatted: English (United States)
Formatted: English (United States)
Formatted: English (United States)
Formatted: English (United States)
Formatted: English (United States)
Formatted: English (United States)
Formatted: English (United States)
Formatted: English (United States)
Formatted: English (United States)
Formatted: English (United States)